NOAA Technical Memorandum NWS WR-229

THE 10 FEBRUARY 1994 OROVILLE TORNADO
A CASE STUDY

Mike Staudenmaier, Jr.
Weather Service Office
Sacramento, California

April 1995

U.S. DEPARTMENT OF COMMERCE / National Oceanic and Atmospheric Administration / National Weather Service

NOAA TECHNICAL MEMORANDA
National Weather Service, Western Region Subseries

The National Weather Service (NWS) Western Region (WR) Subseries provides an informal medium for the documentation and quick dissemination of results not appropriate, or not yet ready, for formal publication. The series is used to report on work in progress, to describe technical procedures and practices, or to relate progress to a limited audience. These Technical Memoranda will report on investigations devoted primarily to regional and local problems of interest mainly to personnel, and hence will not be widely distributed.

Papers 1 to 25 are in the former series, ESSA Technical Memoranda, Western Region Technical Memoranda (WRTM); papers 24 to 59 are in the former series, ESSA Technical Memoranda, Weather Bureau Technical Memoranda (WBTM). Beginning with 60, the papers are part of the series, NOAA Technical Memoranda NWS. Out-of-print memoranda are not listed.

Papers 2 to 22, except for 5 (revised edition), are available from the National Weather Service Western Region, Scientific Services Division, P.O. Box 11188, Federal Building, 125 South State Street, Salt Lake City, Utah 84147. Paper 5 (revised edition), and all others beginning with 25 are available from the National Technical Information Service, U.S. Department of Commerce, Sills Building, 5285 Port Royal Road, Springfield, Virginia 22161. Prices vary for all paper copies; microfiche are $3.50. Order by accession number shown in parentheses at end of each entry.

ESSA Technical Memoranda (WRTM)

2 Climatological Precipitation Probabilities. Compiled by Lucianne Miller, December 1965.
3 Western Region Pre- and Post-FP-3 Program, December 1, 1965, to February 20, 1966. Edward D. Diemer, March 1966.
5 Station Descriptions of Local Effects on Synoptic Weather Patterns. Philip Williams, Jr., April 1966 (Revised November 1967, October 1969). (PB-17800)
8 Interpreting the RAREP. Herbert P. Benner, May 1966 (Revised January 1967).
11 Some Electrical Processes in the Atmosphere. J. Latham, June 1966.
17 A Digitalized Summary of Radar Echoes within 100 Miles of Sacramento, California. J. A. Youngberg and L. B. Overaas, December 1966.
21 An Objective Aid for Forecasting the End of East Winds in the Columbia Gorge, July through October. D. John Coparanis, April 1967.
22 Derivation of Radar Horizons in Mountainous Terrain. Roger G. Pappas, April 1967.

ESSA Technical Memoranda, Weather Bureau Technical Memoranda (WBTM)

25 Verification of Operation Probability of Precipitation Forecasts, April 1966-March 1967. W. W. Dickey, October 1967. (PB-176240)
26 A Study of Winds in the Lake Mead Recreation Area. R. P. Augulis, January 1968. (PB-177830)
28 Weather Extremes. R. J. Schmidli, April 1968 (Revised March 1986). (PB86 177672/AS). (Revised October 1991 - PB92-115062/AS)
29 Small-Scale Analysis and Prediction. Philip Williams, Jr., May 1968. (PB178425)
30 Numerical Weather Prediction and Synoptic Meteorology. CPT Thomas D. Murphy, USAF, May 1968. (AD 673365)
31 Precipitation Detection Probabilities by Salt Lake ARTC Radars. Robert K. Belesky, July 1968. (PB 179084)
32 Probability Forecasting--A Problem Analysis with Reference to the Portland Fire Weather District. Harold S. Ayer, July 1968. (PB 179289)
36 Temperature Trends in Sacramento--Another Heat Island. Anthony D. Lentini, February 1969. (PB 183055)
37 Disposal of Logging Residues Without Damage to Air Quality. Owen P. Cramer, March 1969. (PB 183057)
39 Upper-Air Lows Over Northwestern United States. A.L. Jacobson, April 1969. PB 184296)
40 The Man-Machine Mix in Applied Weather Forecasting in the 1970s. L.W. Snellman, August 1969. (PB 185068)
43 Forecasting Maximum Temperatures at Helena, Montana. David E. Olsen, October 1969. (PB 185762)
44 Estimated Return Periods for Short-Duration Precipitation in Arizona. Paul C. Kangieser, October 1969. (PB 187763)
46 Applications of the Net Radiometer to Short-Range Fog and Stratus Forecasting at Eugene, Oregon. L. Yee and E. Bates, December 1969. (PB 190476)
47 Statistical Analysis as a Flood Routing Tool. Robert J.C. Burnash, December 1969. (PB 188744)
48 Tsunami. Richard P. Augulis, February 1970. (PB 190157)
49 Predicting Precipitation Type. Robert J.C. Burnash and Floyd E. Hug, March 1970. (PB 190962)
50 Statistical Report on Aeroallergens (Pollens and Molds) Fort Huachuca, Arizona, 1969. Wayne S. Johnson, April 1970. (PB 191743)
51 Western Region Sea State and Surf Forecaster's Manual. Gordon C. Shields and Gerald B. Burdwell, July 1970. (PB 193102)
52 Sacramento Weather Radar Climatology. R.G. Pappas and C. M. Veliquette, July 1970. (PB 193347)
54 A Refinement of the Vorticity Field to Delineate Areas of Significant Precipitation. Barry B. Aronovitch, August 1970.
55 Application of the SSARR Model to a Basin without Discharge Record. Vail Schermerhorn and Donal W. Kuehl, August 1970. (PB 194394)
56 Areal Coverage of Precipitation in Northwestern Utah. Philip Williams, Jr., and Werner J. Heck, September 1970. (PB 194389)
57 Preliminary Report on Agricultural Field Burning vs. Atmospheric Visibility in the Willamette Valley of Oregon. Earl M. Bates and David O. Chilcote, September 1970. (PB 194710)
58 Air Pollution by Jet Aircraft at Seattle-Tacoma Airport. Wallace R. Donaldson, October 1970. (COM 71 00017)
59 Application of PE Model Forecast Parameters to Local-Area Forecasting. Leonard W. Snellman, October 1970. (COM 71 00016)
60 An Aid for Forecasting the Minimum Temperature at Medford, Oregon, Arthur W. Fritz, October 1970. (COM 71 00120)
63 700-mb Warm Air Advection as a Forecasting Tool for Montana and Northern Idaho. Norris E. Woerner, February 1971. (COM 71 00349)
64 Wind and Weather Regimes at Great Falls, Montana. Warren B. Price, March 1971.
65 Climate of Sacramento, California. Tony Martini, April 1990. (Fifth Revision) (PB89 207781/AS)
66 A Preliminary Report on Correlation of ARTCC Radar Echoes and Precipitation. Wilbur K. Hall, June 1971. (COM 71 00829)
69 National Weather Service Support to Soaring Activities. Ellis Burton, August 1971. (COM 71 00956)
71 Western Region Synoptic Analysis-Problems and Methods. Philip Williams, Jr., February 1972. (COM 72 10433)
74 Thunderstorms and Hail Days Probabilities in Nevada. Clarence M. Sakamoto, April 1972. (COM 72 10554)
75 A Study of the Low Level Jet Stream of the San Joaquin Valley. Ronald A. Willis and Philip Williams, Jr., May 1972. (COM 72 10707)
76 Monthly Climatological Charts of the Behavior of Fog and Low Stratus at Los Angeles International Airport. Donald M. Gales, July 1972. (COM 72 11140)
77 A Study of Radar Echo Distribution in Arizona During July and August. John E. Hales, Jr., July 1972. (COM 72 11136)
78 Forecasting Precipitation at Bakersfield, California, Using Pressure Gradient Vectors. Earl T. Riddiough, July 1972. (COM 72 11146)
79 Climate of Stockton, California. Robert C. Nelson, July 1972. (COM 72 10920)
80 Estimation of Number of Days Above or Below Selected Temperatures. Clarence M. Sakamoto, October 1972. (COM 72 10021)
81 An Aid for Forecasting Summer Maximum Temperatures at Seattle, Washington. Edgar G. Johnson, November 1972. (COM 73 10150)
82 Flash Flood Forecasting and Warning Program in the Western Region. Philip Williams, Jr., Chester L. Glenn, and Roland L. Raetz, December 1972, (Revised March 1978). (COM 73 10251)
83 A comparison of Manual and Semiautomatic Methods of Digitizing Analog Wind Records. Glenn E. Rasch, March 1973. (COM 73 10669)
86 Conditional Probabilities for Sequences of Wet Days at Phoenix, Arizona. Paul C. Kangieser, June 1973. (COM 73 11264)
87 A Refinement of the Use of K-Values in Forecasting Thunderstorms in Washington and Oregon. Robert Y.G. Lee, June 1973. (COM 73 11276)
89 Objective Forecast Precipitation Over the Western Region of the United States. Julia N. Paegle and Larry P. Kierulff, September 1973. (COM 73 11946/3AS)
91 Arizona "Eddy" Tornadoes. Robert S. Ingram, October 1973. (COM 73 10465)
92 Smoke Management in the Willamette Valley. Earl M. Bates, May 1974. (COM 74 11277/AS)
93 An Operational Evaluation of 500-mb Type Regression Equations. Alexander E. MacDonald, June 1974. (COM 74 11407/AS)
94 Conditional Probability of Visibility Less than One-Half Mile in Radiation Fog at Fresno, California. John D. Thomas, August 1974. (COM 74 11555/AS)
95 Climate of Flagstaff, Arizona. Paul W. Sorenson, and updated by Reginald W. Preston, January 1987. (PB87 143160/AS)
96 Map type Precipitation Probabilities for the Western Region. Glenn E. Rasch and Alexander E. MacDonald, February 1975. (COM 75 10428/AS)
97 Eastern Pacific Cut-Off Low of April 21-28, 1974. William J. Alder and George R. Miller, January 1976. (PB 250 711/AS)
98 Study on a Significant Precipitation Episode in Western United States. Ira S. Brenner, April 1976. (COM 75 10719/AS)
99 A Study of Flash Flood Susceptibility-A Basin in Southern Arizona. Gerald Williams, August 1975. (COM 75 11360/AS)
102 A Set of Rules for Forecasting Temperatures in Napa and Sonoma Counties. Wesley L. Tuft, October 1975. (PB 246 902/AS)
103 Application of the National Weather Service Flash-Flood Program in the Western Region. Gerald Williams, January 1976. (PB 253 053/AS)
104 Objective Aids for Forecasting Minimum Temperatures at Reno, Nevada, During the Summer Months. Christopher D. Hill, January 1976. (PB 252 866/AS)
105 Forecasting the Mono Wind. Charles P. Ruscha, Jr., February 1976. (PB 254 650)
106 Use of MOS Forecast Parameters in Temperature Forecasting. John C. Plankinton, Jr., March 1976. (PB 254 649)
107 Map Types as Aids in Using MOS PoPs in Western United States. Ira S. Brenner, August 1976. (PB 259 594)
108 Other Kinds of Wind Shear. Christopher D. Hill, August 1976. (PB 260 437/AS)
109 Forecasting North Winds in the Upper Sacramento Valley and Adjoining Forests. Christopher E. Fontana, September 1976. (PB 273 677/AS)
110 Cool Inflow as a Weakening Influence on Eastern Pacific Tropical Cyclones. William J. Denney, November 1976. (PB 264 655/AS)
112 The MAN/MOS Program. Alexander E. MacDonald, February 1977. (PB 265 941/AS)
113 Winter Season Minimum Temperature Formula for Bakersfield, California, Using Multiple Regression. Michael J. Oard, February 1977. (PB 273 694/AS)
114 Tropical Cyclone Kathleen. James R. Fors, February 1977. (PB 273 676/AS)
116 A Study of Wind Gusts on Lake Mead. Bradley Colman, April 1977. (PB 268 847)
117 The Relative Frequency of Cumulonimbus Clouds at the Nevada Test Site as a Function of K-Value. R.F. Quiring, April 1977. (PB 272 831)
118 Moisture Distribution Modification by Upward Vertical Motion. Ira S. Brenner, April 1977. (PB 268 740)
119 Relative Frequency of Occurrence of Warm Season Echo Activity as a Function of Stability Indices Computed from the Yucca Flat, Nevada, Rawinsonde. Darryl Randerson, June 1977. (PB 271 290/AS)
121 Climatological Prediction of Cumulonimbus Clouds in the Vicinity of the Yucca Flat Weather Station. R.F. Quiring, June 1977. (PB 271 704/AS)
122 A Method for Transforming Temperature Distribution to Normality. Morris S. Webb, Jr., June 1977. (PB 271 742/AS)
124 Statistical Guidance for Prediction of Eastern North Pacific Tropical Cyclone Motion - Part I. Charles J. Neumann and Preston W. Leftwich, August 1977. (PB 272 661)
125 Statistical Guidance on the Prediction of Eastern North Pacific Tropical Cyclone Motion - Part II. Preston W. Leftwich and Charles J. Neumann, August 1977. (PB 273 155/AS)
126 Climate of San Francisco. E. Jan Null, February 1978. Revised by George T. Pericht, April 1988. (PB88 208624/AS)
127 Development of a Probability Equation for Winter-Type Precipitation Patterns in Great Falls, Montana. Kenneth B. Mielke, February 1978. (PB 281 387/AS)
128 Hand Calculator Program to Compute Parcel Thermal Dynamics. Dan Gudgel, April 1978. (PB 283 080/AS)
129 Fire whirls. David W. Goens, May 1978. (PB 283 866/AS)
130 Flash-Flood Procedure. Ralph C. Hatch and Gerald Williams, May 1978. (PB 286 014/AS)
131 Automated Fire-Weather Forecasts. Mark A. Mollner and David E. Olsen, September 1978. (PB 289 916/AS)
132 Estimates of the Effects of Terrain Blocking on the Los Angeles WSR-74C Weather Radar. R.G. Pappas, R.Y. Lee, B.W. Finke, October 1978. (PB 289767/AS)
133 Spectral Techniques in Ocean Wave Forecasting. John A. Jannuzzi, October 1978. (PB291317/AS)
134 Solar Radiation. John A. Jannuzzi, November 1978. (PB291195/AS)
135 Application of a Spectrum Analyzer in Forecasting Ocean Swell in Southern California Coastal Waters. Lawrence P. Kierulff, January 1979. (PB292716/AS)
136 Basic Hydrologic Principles. Thomas L. Dietrich, January 1979. (PB292247/AS)
137 LFM 24-Hour Prediction of Eastern Pacific Cyclones Refined by Satellite Images. John R. Zimmerman and Charles P. Ruscha, Jr., January 1979. (PB294324/AS)
138 A Simple Analysis/Diagnosis System for Real Time Evaluation of Vertical Motion. Scott Heflick and James R. Fors, February 1979. (PB294216/AS)
139 Aids for Forecasting Minimum Temperature in the Wenatchee Frost District. Robert S. Robinson, April 1979. (PB298339/AS)
140 Influence of Cloudiness on Summertime Temperatures in the Eastern Washington Fire Weather district. James Holcomb, April 1979. (PB298674/AS)
141 Comparison of LFM and MFM Precipitation Guidance for Nevada During Doreen. Christopher Hill, April 1979. (PB298613/AS)

NOAA Technical Memorandum NWS WR-229

THE 10 FEBRUARY 1994 OROVILLE TORNADO
A CASE STUDY

Mike Staudenmaier, Jr.
Weather Service Office
Sacramento, California

April 1995

UNITED STATES
DEPARTMENT OF COMMERCE
Ronald H. Brown, Secretary

National Oceanic and
Atmospheric Administration
D. James Baker, Under Secretary
and Administrator

National Weather Service
Elbert W. Friday, Jr., Assistant
Administrator for Weather Services

This publication has been reviewed
and is approved for publication by
Scientific Services Division,
Western Region

Delain A. Edman, Chief
Scientific Services Division
Salt Lake City, Utah

TABLE OF CONTENTS

TABLE OF FIGURES

THE 10 FEBRUARY 1994 OROVILLE TORNADO: A CASE STUDY

Mike Staudenmaier, Jr.
National Weather Service Office
Sacramento, California

ABSTRACT

An F2 tornado touched down in the northern portion of the Sacramento Valley on 10 February 1994 causing significant damage in Oroville, California. This study documents the event and explores the possibility that the storm had supercellular structures including a mesocyclone. A collision of mesoscale boundaries interacting in a low buoyancy environment acted as the focus for the development of the thunderstorm. A strong barrier jet along the west side of the Sierra Nevada acted to create strong storm-relative helicity in this environment. Dry air rotating around the base of an upper-level trough acted to destabilize the atmosphere allowing for an enhancement of the convection. The orientation of the Sacramento Valley is such that strong storm-relative helicity can be created, under certain synoptic conditions, which is sufficient to develop rotation in developing thunderstorms. Rotation was detected in the mid levels of this storm and was likely responsible for the development of the damaging F2 tornado.

I. INTRODUCTION

On 10 February 1994, strong thunderstorms developed in the northern Sacramento Valley. At approximately 2230 UTC, an F2 tornado (damage survey by Weather Serice Office (WSO) Redding) touched down near Oroville, California (see Fig. 1 for locations). This tornado was associated with a small complex of thunderstorms which developed explosively around 2200 UTC after a cold frontal passage aloft. Due to the unique topography found in the Sacramento Valley, these thunderstorms encountered an environment supportive of supercellular development with strong low-level wind shear. Although the instability was not extreme, this wind shear was sufficient to develop an F2 tornado which damaged 37 homes and injured one person in the town of Oroville. Remarkably, the tornado was estimated to have only spent between 40 to 60 seconds on the ground with a path width of 10 to 20 yards.

Most northern and central California tornadoes occur after a strong, cold frontal passage aloft. Thus, the environment of storm genesis is located in the cold sector of the storm, characterized by low buoyancy. Most California tornadoes were thought to be mainly touchdowns of cold air funnels, but recent studies have shown that some of the larger tornadoes which have occurred in California may have been mesocyclone induced (Braun and Monteverdi 1991; Monteverdi and Quadros 1994). McCaul (1990, 1991) has shown that supercellular convection can even occur in low-buoyancy environments from internally generated pressure perturbations associated with tropical storms with significant low-level wind shear. Thus, if a favorable ambient wind shear profile is present, mesocyclone-induced

tornadogenesis can occur even in a low buoyancy environment such as the cold sector of a synoptic-scale storm. Hales (1985) has shown that topography can create a shear profile favorable for supercellular convection in the Los Angeles Basin. Braun and Monteverdi (1991) have shown that channeling effects in the Sacramento Valley can produce wind shear profiles favorable for supercellular convection.

When the location of California tornado occurrence is investigated, a few areas of the Central Valley appear more favorable to tornadic development. Figure 2, which shows tornado touchdowns between 1961 and 1991, illustrates that the northern Sacramento Valley clearly has a localized maximum of tornado touchdowns over southern Tehama County and Butte and Glenn Counties. South of this region in the southern Sacramento Valley, only a few touchdowns have been recorded. Much of the San Joaquin Valley has had tornado touchdowns, however no discernable spacial pattern is evident.

Over the last 10 years, many technological advancements have been made in the National Weather Service software programs which diagnose the current atmospheric patterns, giving forecasters a better estimate of what to expect in the short term. This has greatly improved the ability of forecasters to determine severe weather potential and to forecast areas which are likely to see damaging thunderstorms. This paper will examine two of the new advancements, the Skew-T/Hodograph Analysis and Research Program, or SHARP (Hart and Korotky 1991), and the usefulness of PC-GRIDDS in manipulating gridded data. These programs will be used to diagnose the conditions that led to the Oroville tornado.

All of these topics will be investigated further in this study. Primarily, this study will illustrate the conditions which led to the development of the Oroville tornado. The usefulness of both PC-GRIDDS and the SHARP Workstation in determining areas of severe weather potential and forecasting the likely character of severe weather for this case will also be examined. This study will compare the environment of the Oroville tornado with the results from other studies of California tornadoes in order to add to the sparse body of literature on severe thunderstorms in California. Finally, the apparent tornado maximum in the northern Sacramento Valley will be investigated further.

II. ANTECEDENT CONDITIONS OF THE OROVILLE TORNADO

By 1200 UTC 10 February 1994, an environment supportive of severe thunderstorms was developing over the northern portion of the Sacramento Valley. A moderately strong mid- and upper-level cold front was located to the west of California. This system had moved southward from the Gulf of Alaska, a track typical of "high latitude" cyclones (Weaver 1962). There was very little surface reflection to this system. This is typical of frontal systems which are in their later stages of evolution. This type of frontal structure is common in the western United States, western Europe, and the United Kingdom and usually consists of a sharp moisture discontinuity aloft with little surface reflection (Browning and Monk 1982). Located behind this upper-level cold front were open-celled cumulus indicating the cold pool aloft and the instability of the airmass behind the front. This cumulus field showed greatest enhancement under the left front quadrant of an advancing jet streak aloft.

Due to the topography of the Sacramento Valley, the general overall synoptic pattern, and a strong ageostrophic secondary circulation around an upper-level jet streak, a southerly low-level barrier jet was likely present. The low-level barrier jet in the Sacramento Valley has been researched by Parish (1982) and was found to occur between 1200-4500 feet above ground level when a cold front and/or upper-level trough approached the mountains from the west (Fig. 3). The cross-mountain flow which develops over the Sacramento Valley is initially statically stable and becomes dammed against the east side of the valley creating the low-level barrier jet. On 10 February 1994, the barrier jet was likely enhanced significantly by the secondary circulations of the strong jet streak aloft. Unfortunately, wind profiler data was not available for this day, but the barrier jet has been seen on other days when similar conditions have prevailed (Fig. 4). Below the radiation inversion, surface winds were generally southeasterly at around 10-15 mph but were forecast to increase through the day as the upper system moved onshore and tightened the surface pressure gradient.

In the mid and upper levels, strong positive vorticity advection (PVA) increasing in height was occurring over northern California (Fig. 5). This PVA was expected to increase through the afternoon. A 20 X 10^{-6} s^{-1} unit absolute vorticity center, at the 500 mb level, was located about 200 miles west of the California coast and was forecast to be over northern California by 0000 UTC 11 February (Fig. 6). Isentropic and orographic lift were also strengthening through the day as seen in the time cross-section for the Oroville region (Fig. 7). Synoptic-scale lifting generally acts to destabilize the atmosphere, by lowering the level of free convection. This increases the environmental lapse rate which increases the positive buoyancy of a parcel.

Strong cold air advection was occurring into the base of the trough indicating that the trough would deepen as it moved eastward (Fig. 8). 500 mb temperatures of less than -30.0°C were located in the base of the trough. In advance of the trough at lower levels, weak warm air advection was occurring over California with 850 mb temperatures greater than +5.0°C. Since this area of very cold temperatures aloft was forecast to propagate over northern California, becoming vertically collocated with the area of warm air advection at the lower levels, a sharp decrease in stability was expected to occur.

Due to the baroclinicity with this system, strong winds were located at all levels, but were especially concentrated west of the trough axis. A speed maximum was forecast to rotate through the base of the trough and propagate over central California by 0000 UTC. This would create a large area of synoptic lift in the mid-troposphere over most of northern California. At 1200 UTC, wind speeds of greater than 100 knots at 300 mb (Fig. 9) and greater than 40 knots at 850 mb (Fig. 10) emphasized the strength of this system.

The vertical wind profile plays an important role in determining what type of severe weather may occur. However, it is not something quickly or easily calculated from a glance at a Skew-T/log-P diagram. An examination of an observed or modified hodograph will indicate in which kind of environment a storm will develop. Weisman and Klemp (1982), among others, have shown that a low-level wind veering and increasing with height is a necessary criteria for the development of long-lived rotating thunderstorms. The low-level wind shear vectors, particularly in the

lowest 3 km, should appear curved in a clockwise sense (i.e., veer with height) on the hodograph. In these situations, the tilting of horizontal vorticity into the vertical is maximized and high values of helicity are produced. Davies-Jones et al. (1990) found that a 0-3 km storm-relative helicity value approaching 150 m^2/s^{-2} generally supported mesocyclone development. A value of 151-299 m^2/s^{-2} supported weak tornadoes; while a value of 300-499 m^2/s^{-2} supported strong tornado development. These should not be taken as rigid boundaries, but rather very general guidelines to tornadic activity. If the hodograph is a straight line, multicellular development is likely. As previously stated, it has been shown that marginal instabilities, as estimated by CAPE, or Convective Available Potential Energy, may be associated with strong to severe tornadoes if they are coincident with high values of storm-relative helicity.

Weisman and Klemp (1982, 1984) have also shown that much of the relationship between storm type, wind shear, and buoyancy can be represented in the form of a Bulk Richardson Number, R, defined to be

$$R = \frac{B}{1/2\ U^2}$$

where B is the buoyant energy in the storm's environment (or CAPE) and U is a measure of the vertical wind shear. U is calculated by taking the difference between the density-weighted mean wind over the lowest 6 km and a representative surface layer wind (500 m mean wind). The numerical modeling results of Weisman and Klemp (1982, 1984) and calculations of R for a series of documented storms both suggest that unsteady, multicellular growth occurs most readily for R > 30 and that supercellular growth is confined to magnitudes of R between 10 and 40. However, while ratios of buoyancy to shear might suggest that rotation is possible within a storm, tornadic potential can be realized only for those cases where the synoptic and mesoscale environments are supportive for the development of thunderstorms for a long enough period of time.

The Oakland, CA (OAK) sounding from 1200 UTC indicated a thick, moist layer extending from the surface to 825 mb (Fig. 11). This was capped by a dry, more stable layer between 825 mb and 800 mb. From 800 mb to 575 mb, the lapse rate approached moist adiabatic, with dry air located above 575 mb. The low levels of the OAK sounding were similar to the Sacramento low-level sounding, thus it provided a good proximity sounding for the Sacramento Valley. The Lifted Index at 500 mb was +6.0°C, but was +2.0°C at 700 mb, indicating that most of the buoyant energy available for storm development would be located below 500 mb. The wind profile in the OAK sounding was missing for the lowest 3000 feet, but likely indicated some veering with height since the wind was light southeasterly at the surface but southwesterly above 900 mb. However, in the valley, due to the barrier jet, significant veering with height was occurring in the vertical wind profile.

The Medford, OR (MFR) sounding for the same time period indicated a much thicker moist layer extending up to 700 mb before encountering the remnants of the dry and warm layer (Fig. 12). The fact that this dry layer has been lifted significantly higher at MFR indicated that the moist layer increased in depth towards the north, and that stronger, more persistent, synoptic lift along with dynamic destabilization was occurring at MFR. The wind profile for MFR showed some turning of the wind, but nothing of any significance.

III. ANALYSIS AND STORM EVOLUTION

Gridded data from the 1200 UTC Eta model run indicated that strong PVA was to move over the region throughout the day, as the cold core system moved onshore. Of more importance for the severe weather threat, however, was the dry air intrusion which was shown to be advecting into the region over the next 12 hours (Figs. 13-14). This area of low equivalent potential temperature air was also apparent in the water vapor imagery, as a dry slot on the west side of the trough. A PC-GRIDDS-derived Q-vector field of the 850-400 mb layer indicated a large area of implied ascent in the mid-troposphere over northern California (Fig. 15). This thermal imbalance and its associated ascent, would lead to destabilization over this region.

The six-hour forecasted gridded data field valid at 1800 UTC indicated that parts of California were becoming very conducive to the development of thunderstorms. The 280K isentropic surface indicated an area of strong isentropic rising motion from northeastern California to southeastern California (Fig. 16). When the 286K-306K atmospheric column was investigated, an area of weak static stability was found from southwestern Idaho across northern California to south of San Francisco (Fig. 17). When adiabatic moisture flux convergence was investigated, an area of dynamic destabilization could be seen over northern and eastern California as well (Fig. 18). This area was destabilizing as warm moist air forced isentropes apart due to convergence of mass. Pressure advection at the 282K isentropic level indicated the upward velocities were occurring over northern and eastern California (Fig. 19). This broad area of rising motion in the lowest levels contributed to increasing the lapse rate over this region and destabilizing the airmass further. Although the strongest areas of pressure advection and adiabatic moisture flux convergence were occurring south of the Oroville area at 1800 UTC, it is likely that much of this unstable airmass in the lower atmosphere was being advected northward due to the barrier jet on the east side of the valley.

Satellite imagery at this time (not shown) indicated that the cold front was propagating across northern California. The frontal band of cloudiness associated with the front was pushing southward across central California ahead of the advancing front. This was allowing insolation to occur over northern California causing destabilization to occur. Although the topography was destroying the baroclinicity of the front in the lower levels, the upper-level front remained strong.

A normalized cross-section from 48°N 128°W to 30°N 117°W at 1800 UTC indicated that strong secondary circulations were located underneath the jet streak aloft over the area of concern (Fig. 20). Strong southeasterly flow was occurring at the surface likely contributing to the strong south to southeasterly barrier jet. Thus, isallobaric contributions from the rapidly deepening surface low and strong secondary circulations due to the jet streak aloft were both enhancing the southerly flow in the Sacramento Valley ahead of the approaching system.

At 1900 UTC, the sub-synoptic analysis indicated that a weak pressure trough extended northward through the middle of the Sacramento Valley (Fig. 21). This pressure trough in the valley had been documented in other case studies as well (Weaver 1962; Braun and Monteverdi 1991; Monteverdi 1993). Of significant note were the strong southeasterly winds on the eastern side of the valley. Sustained winds

of greater than 20 mph with gusts approaching 30 mph indicated that momentum from the barrier jet was mixing down to the surface. Additional accelerations were being forced by the isallobaric component of the wind. Dewpoints in this region were rapidly approaching 50°F or more, further decreasing the convective stability over this area.

South of Redding, a strong windshift/moisture discontinuity could be identified. This feature was moving toward the southeast and was probably forced by terrain channeling of the geostrophic upper-level winds. Whiteman and Doran (1993) have investigated the relationship between valley and ridgetop wind directions and identified four different mechanisms for their relationship. Of the four, terrain channeling was likely the most important parameter in terms of the development of this windshift/moisture discontinuity. In their study, Whiteman and Doran (1993) found that in certain situations a small wind shift aloft can lead to a 180 degree wind shift at the valley floor due to terrain channeling. Since this channeling forces the low-level wind in a valley to take on the component of the upper-level wind that is parallel to the valley, the strong southwesterly flow ahead of the cold front was producing strong southerly flow in the valley. However, west to northwest flow was located behind the cold front. Thus, as the front propagated over California, a strong windshift line developed at the north end of the valley and propagated southward with the upper-level front. Due to downslope flow and subsidence, this northerly wind was also very dry, with dewpoint temperatures in the 30s. Thus, a moisture discontinuity was created as well as a windshift line.

The 2000 UTC analysis indicated that the windshift/moisture discontinuity had moved farther south, pushing through the Red Bluff area (Fig. 22). Thunderstorms were forming at the triple point between the surface windshift line and the valley pressure trough near Red Bluff. The dewpoint temperature at Chico (CIC) was now 54°F with winds gusting to 20 mph from the southeast while Red Bluff had a dewpoint temperature of 49°F and falling, with winds from the west at 10 mph. Stronger surface winds were developing as the surface pressure gradient became stronger across the southern portion of the Sacramento Valley. Thus, significant moisture convergence was occurring along this windshift line as it moved into the more unstable airmass to the south.

At 2005 UTC, a funnel cloud was reported over Tehama County. This funnel cloud was very short-lived, and was likely a cold-air funnel developing as the cold equivalent potential temperature minimum air aloft continued to destabilize the atmosphere. At this time, satellite imagery indicated significant clearing occurring across the northern Sacramento Valley as the upper-level front continued to propagate southeastward over California.

By 2100 UTC, water vapor satellite imagery clearly indicated the dry slot advecting around the base of the trough and pushing over the triple point at the surface (Fig. 23). This was the dry air that was evident in the 1200 UTC MFR sounding. Visible satellite imagery (Fig. 24) indicated that significant clearing had occurred allowing for solar insolation to continue to rapidly destabilize the airmass over the northern Sacramento Valley. Although hard to see in this image, a thin line was beginning to form along the windshift line as thunderstorms rapidly developed from northeast to southwest. The surface analysis at this time indicated strong southeasterly flow into the region of the triple point which represented increasing

moisture convergence and strong baroclinic surface vorticity at that location (Fig. 25). Oroville had a dewpoint temperature of 51°F with 25 mph sustained winds from the southeast. The pressure gradient continued to strengthen over this area as solar insolation decreased the pressure over the northern portion of the valley, and cloud cover remained over the southern portion. A secondary push of drier air had formed on the west side of the valley and was now propagating northeastward as evident from the wind shift from southerly to westerly and the dewpoint drop of 2°F at Brooks (BSS).

By 2200 UTC, a large anvil was covering the northern Sacramento Valley as a large thunderstorm rapidly developed along the triple point. As will be seen later, this storm was now in a region of significant low-level shear with a Bulk Richardson Number less than 15. Chico (CIC) reported a windshift at the time of observation as the windshift line, or possibly the gust front, began to move through the city (Fig. 26). Towering cumulus were being reported north through southeast as thunderstorms began to develop southward along the Sierra Nevada foothills. However, the thunderstorm to the north of CIC was dominating the local environment as many of the other thunderstorms began to weaken due to the upper-level subsidence forced by this rapidly growing thunderstorm. As the near-surface air was lifted by the gust front, it likely began rotating in the high helicity environment near CIC, ultimately developing into a mesocyclone.

At 2228 UTC, the Redding WSO received a phone call from the California Department of Forestry (CDF) Headquarters in Oroville reporting that they were "looking at a tornado out their window". The National Weather Service at Sacramento was called for radar confirmation, but the WSR-57 radar only indicated VIP level 2 in the vicinity of Oroville (Fig. 27). Of greater importance however, was the WSR-88D Doppler radar which indicated a weak circulation in the mid and upper levels of the storm likely indicative of a developing mesocyclone. This rotation was seen by meteorologists working at WSO Sacramento (SAC) that afternoon. Unfortunately, only one velocity image was archived, as testing of the radar was occurring at the same time. This 2.4° scan of velocity indicated strong storm top divergence occurring with this storm (Fig. 28). Since the storm was about 60 miles away, the beam of the radar was slicing through the storm at the 18,500 foot level which was close to the storm top of 22,000 feet. Satellite imagery (not shown) indicated a "V-notch" signature which also remarks on the strength of the storm and the upper-level divergence.

By 2300 UTC, the surface analysis showed that the outflow boundary was propagating to the east-southeast (Fig. 29). While the storm was moving to the southeast, the actual tornado path was to the northeast. This possibly occurred during the meso-occlusion stage of the mesocyclone. As the storm reached the Sierra Nevada foothills, it took a more eastward track, as did the dissipating tornado (as witnessed by an observer located east of Oroville). The tornado dissipated soon afterward.

Another interesting occurrence between 2200 and 2300 UTC was a polarity switch in cloud-to-ground lightning reported by the BLM Lightning Detection Network. Before 2200 UTC, only negative strikes were occurring, however between 2230 and 2300 UTC, only one positive strike occurred (and no negative strikes). After 2300 UTC, more negative strikes were reported. This polarity switch in tornadic storms has been documented in other cases

as well (Branick and Doswell 1992; Curran and Rust 1992).

A sounding representing the local environment of the Oroville tornado was created by using the gridded model data from the 1200 UTC Eta model run and interpolating the temperature and dewpoint data for the mandatory levels with the 12 hour forecast for 0000 UTC 11 February (Fig. 30). This was to simulate what was available to forecasters that morning. These data were entered into the SHARP Workstation and the surface was modified to represent the surface pressure of Oroville, adjusting for the temperature and dewpoint which was expected to occur. The winds were also adjusted to represent the southerly low-level barrier jet in the valley and the strong west to northwesterly winds located aloft.

This sounding clearly indicated that the environment was conducive to the development of supercellular type storms. A Bulk Richardson Number of 11 combined with a 0-3 km storm-relative helicity value of 355 m^2/s^{-2}, using the storm motion vector from 321° at 19 kts, suggest that developing storms could have complex structures with supercellular characteristics (Weisman and Klemp 1982; Davies-Jones 1990). The CAPE was calculated to be near 750 J/kg which was not highly unstable, but as previously stated, with high helicity values, large instability is not needed for tornadogenesis (McCaul 1990). Storm-relative inflow in this environment was from the southeast at 40-45 knots, which verifies the strong convergence which was assumed from the sub-synoptic analyses. The Lifted Index at the 500 mb level at this time was -3.0°C, but at 700 mb was -4.0°C. The hodograph was indicative of a veering of the wind with height in the lower troposphere with northwest winds above this (Fig. 31).

Gridded data at 0000 UTC indicated that at the 250 mb level, a large area of cyclonic vorticity advection was occurring over northern California juxtaposed with an area of warm air advection (Fig. 32). This was leading to strong height falls at the surface and a rapid deepening of the surface low from 1020 mb at 1200 UTC to 1008 mb at 0000 UTC. This rapid deepening created strong southerly isallobaric winds across most of eastern California. Associated with this strong area of warm air advection and cyclonic vorticity advection was a tropopause fold in the upper troposphere. This tropopause fold can be seen in a equivalent potential temperature temporal cross-section as 362K stratospheric air replaces 340K tropospheric air (Fig. 33). Strong rising motion ahead of this tropopause fold suggests the strength of this upper system. As discussed by Hirschberg and Fritsch (1991, 1993), thermal advections in the vicinity of tropopause undulations can be quite large and will have a great effect on height tendency in the lower atmosphere and its associated vertical velocity. Of additional note was the stable layer present at 1200 UTC between 800 mb and 500 mb which was forced upward to a position between 600 mb and 400 mb by 0000 UTC by these vertical motions. This was the dry, stable layer which was present in the OAK and MFR soundings from 1200 UTC and at 0000 UTC. Under this dry stable layer was a moist unstable area, and as the dry stable layer was lifted, dynamic destabilization in the lower levels increased the depth of the moist unstable layer. The dry air intrusion could be seen occurring from 09 hours (2100 UTC) to 30 hours as low equivalent potential temperature air advected into the region. This air was not much cooler than the air it was replacing, thus the decrease in equivalent potential temperature was due mainly to a lack of moisture. This feature was the upper-level front discussed earlier.

A cross-section from 36°N 132°W to 40°N 112°W at 0000 UTC indicated that the strong rising motions in the secondary circulations had decreased (Fig. 34). A strong outflow from the upper-level jet could be seen at the 200-300 mb layer near the jet streak and tropopause fold. The strong secondary circulations seen in the near-surface layer earlier had weakened significantly. Although the airmass behind the cold front was unstable, as seen in the low values of equivalent potential temperature by 0000 UTC, there was a very strong cap between 700 and 500 mb which was prohibiting any convective instability from being realized.

IV. TORNADO OCCURRENCE IN THE NORTHERN SACRAMENTO VALLEY

As previously stated, it appears that certain areas of the northern Sacramento Valley are more prone to thunderstorms which may take on supercellular structures. These storms are responsible for a maximum of tornadic activity over areas of southern Tehama County and Butte and Glenn Counties. South of this region there are relatively few recorded tornado touchdowns. A possible explanation for this is a lack of population centers between Red Bluff, in Tehama County, and Sacramento. However, the relative flatness of the land and the abundance of agriculture in the Sacramento Valley would suggest that tornadoes should have a good chance of detection by agricultural workers. Damage would likely be noticed by them after the storm was over, even if the tornado was not seen. Also, many small communities have developed across this region over the last ten years adding to the potential for tornado sightings.

More likely, however, is that the maximum in tornado occurrence over the northern Sacramento Valley is due to meteorological forcing, such as the existence of a barrier jet developing along the east side of the valley and a maximum of convergence between the valley trough and southeastward moving windshift lines, often associated with upper-level fronts. Additional convergence is likely over the northeastern portion of the Sacramento Valley as the Sierra Nevada Mountains extend further westward and Sutter Buttes rise out of the valley floor.

Parish (1982) has found that low-level mountain parallel jets are a common wintertime and early springtime feature along the western slope of the Sierra Nevada Range. He proposes that the development of the barrier jet occurs whenever a large-scale component of wind is directed towards a mountain chain causing the air to be forced to rise over the barrier. If the air has a high static stability, the forced ascent is resisted and appreciable deceleration occurs. This leads to the damming of stable air against the mountains and consequently an increase in pressure along the windward slopes. The resulting damming leads to a pressure gradient force strikingly dissimilar to the large-scale conditions, being directed away from the mountains. If such conditions persist for periods of time exceeding a few hours, Coriolis effects become important. The local pressure field will then support southerly geostrophic-type motion parallel to the mountains. Of course, friction and diabatic effects must also be considered, but their combined effect is not as easily calculated. It was found that the strongest winds were located 600-1500 m above ground level, with a horizontal extent of at least 100 km, reaching down into the California Valley. He found that much weaker winds existed at the surface below the radiative inversion. Occasionally, a valley trough formed with westerly winds located on the west side, in striking

contrast with the surface pressure gradient.

Another reason for a preferred area of thunderstorm development over the northern Sacramento Valley is the climatological location of the triple point formed between the valley trough and a southeastward moving windshift line associated with terrain channeling of the ridgetop winds. As this windshift line moves southeastward, a collision between it and the valley trough will occur over the northern portion of the Sacramento Valley. It has been shown that the collision between two boundaries is a preferred region for the development of strong to severe thunderstorms (Doswell 1985). This was likely the genesis mechanism for the Oroville thunderstorm. The near-surface moist flow was vertically stretched as it accelerated upward and began rotating in the high helicity environment in the lower levels which likely caused the Oroville thunderstorm to develop into a severe storm.

The orientation of the valley leads to a gradient of Bulk Richardson Number across the valley. Bulk Richardson Numbers will decrease from west to east due to the increasing shear found on the east side arising from the barrier jet (assuming storm motion from a northerly direction). The shear is likely increased through compression on the east side of Sutter Buttes and the merging of the valley walls at the north end of the valley. All of this leads to the lowest Bulk Richardson Numbers on the east side of the valley, likely within the values supportive of supercellular development as defined by Weisman and Klemp (1982).

All of these factors lead to an area in the northern Sacramento Valley which appears to be more prone to storms which may take on supercellular structures. Due to the finite width of the valley, many of these storms will likely develop rotation briefly, if at all, and quickly return to a multi-cellular structure when the foothills are reached. Also, due to the post frontal environment, storm tops are usually below 30,000 feet, thus limiting the extent to which they can be examined by Doppler radar. Thus, these storms take on characteristics similar to the early stages of supercells in the Midwest, but never have enough time or instability to develop into the much more powerful supercells which plague that region.

V. DISCUSSION AND CONCLUSION

The northern Sacramento Valley is an area where interactions between a valley-induced pressure trough and a strong windshift line climatologically occur. General convergence occurs here, as well, due to a confluence of the valley walls. A high occurrence of thunderstorm echoes over this region, which are likely due to this phenomena, can be seen in the WSR-57 radar data archive (WSO-SAC).

A strong southerly barrier jet which develops along the east side of the Sacramento Valley during the winter causes strong moisture convergence to occur as well. Previous studies of California tornadoes (Hales 1985; Braun and Monteverdi 1991; Monteverdi and Quadros 1994) support the theory that shear profiles favorable for storm rotation can be created by topography in California. In the Oroville case study, this strong southerly flow transported high moisture values northward along the east side of the valley-induced pressure trough. This moist flow impinged on the southeastward moving windshift line and was forced upward. Strong thunderstorms developed as a midlevel dry push advected over the

area adding to the destabilization. This occurred in an environment which was being destabilized by solar insolation due to the midlevel dry push behind the upper-level front. The near-surface moist flow was vertically stretched as it accelerated upward and began rotating in the high helicity environment in the lower levels which likely caused the Oroville thunderstorm to develop into a severe storm.

This study has explored the uses of the SHARP Workstation and PC-GRIDDS in determining the area of severe weather potential on 10 February 1994. The Oroville tornado was a good example of how certain storms may behave under optimum conditions over the northern Sacramento Valley. The Oroville storm appeared to contain brief supercellular structures. These structures, including mesocyclones and moderately strong tornadoes, can develop due to high values of valley-induced storm-relative helicity which can support tornadogenesis even within the post-frontal, low buoyancy environment. This study shows how important it is for forecasters to be aware of the mesoscale processes which occur in their forecast area and to realize when the interaction between the mesoscale and the synoptic scale can lead to the development of severe thunderstorms and tornadoes. With the implementation of the WSR-88D Doppler radar in Sacramento, it is likely that this type of thunderstorm will be detected and investigated more closely in the future.

Acknowledgments. The author expresses his gratitude to the offices of WSO Redding and WSO Sacramento for their support and information. Correspondence with John Monteverdi was very useful in comparing theories and ideas. I would especially like to thank SOO Scott Cunningham, Dan Baumgardt, and the Western Region Scientific Services Division for their time in reviewing this paper. Their useful suggestions and comments have solidified the science of this paper.

VI. REFERENCES

Barnes, S., 1985: Omega diagnostics as a supplement to LFM/MOS guidance in weakly forced convective situations. *Mon. Wea. Rev.*, **113**, 2122-2141.

_____, 1986: On the accuracy of omega diagnostic computations. *Mon. Wea. Rev.*, **114**, 1664-1680.

Bluestein, H.B., 1986: Fronts and jet streaks: a theoretical perspective. *Mesoscale Meteorology and Forecasting,* Peter Ray, Ed., Amer. Meteor. Soc., 173-215.

Branick, M.L., and C.A. Doswell III, 1992: An observation of the Relationship between supercell structure and lightning ground-strike polarity. *Wea. Forecasting*, **7**, 143-149.

Braun, S.A. and J.P. Monteverdi, 1991: An analysis of a mesocyclone-induced tornado occurrence in Northern California. *Wea. Forecasting*, **6**, 13-31.

Browning, K.A., and G.A. Monk, 1982: A simple model for the synoptic analysis of cold fronts. *Quart. J. R. Met. Soc.*, **108**, 435-452.

Curran, E.B., and W.D. Rust, 1992: Positive ground flashes produced by low-precipitation thunderstorms in Oklahoma on 26 April 1984, *Mon. Wea. Rev., **120***, 544-553.

Cooley, J., 1978: Cold air funnel clouds. *Mon. Wea. Rev.*, **106**, 1368-1372.

Davies-Jones, R.D., Burgress and M. Foster, 1990: Test of helicity as a tornado forecast parameter. *16th AMS Conference on Severe Local Storms*, Kananaskis Park, Alberta, 588-592.

Doswell, C.A. III, 1985: The operational meteorology of convective weather Volume II: Storm scale analysis. 240 pp. NOAA Tech. Memo. ERL ESG-15.

Hales, J., 1985: Synoptic features associated with Los Angeles tornado occurrences. *Bull. Amer. Meteor. Soc.*, **66**, 657-662.

Hart, J.A. and J. Korotky, 1991: The SHARP workstation--A Skew T/Hodograph analysis and research program. NOAA/NWS NWSFO Charleston.

Hirschberg, P.A. and J.M. Fritsch, 1991: Tropopause undulations and the development of extratropical cyclones. Part I: Overview and observations from a cyclone event. *Mon. Wea. Rev.*, **119**, 496-517.

_____, 1993: On understanding height tendency. *Mon. Wea. Rev.*, **121**, 2646-2661.

Johns, R.H. and C.A. Doswell III, 1992: Severe local storms forecasting. *Wea. Forecasting*, **7**, 588-612.

Kloth, C.M., and R.P. Davies-Jones, 1980: The relationship of the 300 mb jet stream to tornado occurrence. NOAA Tech. Memo. ERL NSSL-88, Nat'l Severe Storms Lab., Norman OK, 62 pp.

Leftwich, P.W., and X. Wu, 1988: An operational index of the potential for violent tornado development. Preprints: *15th Conference on Severe Local Storms,* Boston, Amer. Meteor. Soc., 472-475.

McCaul, E.W., Jr., 1990: Simulations of convective storms in hurricane environments. *16th AMS Conference on Severe Local Storms*, Kananaskis Park, Alberta, 334-339.

_____, 1991: Buoyancy and shear characteristics of hurricane-tornado environments. *Mon. Wea. Rev.*, **119**, 1954-1978.

McNulty, R.P, 1978: On upper tropospheric kinematics and severe weather occurrence. *Mon. Wea. Rev.*, **106**, 662-672.

Monteverdi, J.P., 1993: A case study of the operational usefulness of the SHARP workstation in forecasting a mesocyclone-induced cold sector tornado event in California. *NOAA Technical Memorandum.* NWS WR-219. 22 pp.

_____, and J. Quadros, 1994: Convective and rotational parameters associated with three tornado episodes in Northern and Central California. (in press).

Moore, J.T., and G.E. VanKnowe, 1992: The effect of jet-streak curvature on kinematic fields. *Mon. Wea. Rev.*, **120**, 2429-2441.

Parish, T.R., 1982: Barrier winds along the Sierra Nevada Mountains. *J. Appl. Meteor.*, **21**, 925-930.

Weaver, R.L., 1962: Meteorology of hydrologically critical storms in California. U.S. Weather Bureau, Hydrologic Services Division, Hydrol. Rep. No. 37, Washington, D.C., 207 pp.

Weisman, M.L., and J.B. Klemp, 1982: The dependence of numerically simulated convective storms on vertical shear and buoyancy. *Mon. Wea. Rev.*, **110**, 504-520.

Whiteman, C.D., and J.C. Doran, 1993: The relationship between overlying synoptic-scale flows and winds within a valley. *J. Appl. Meteor.*, **32**, 1669-1682.

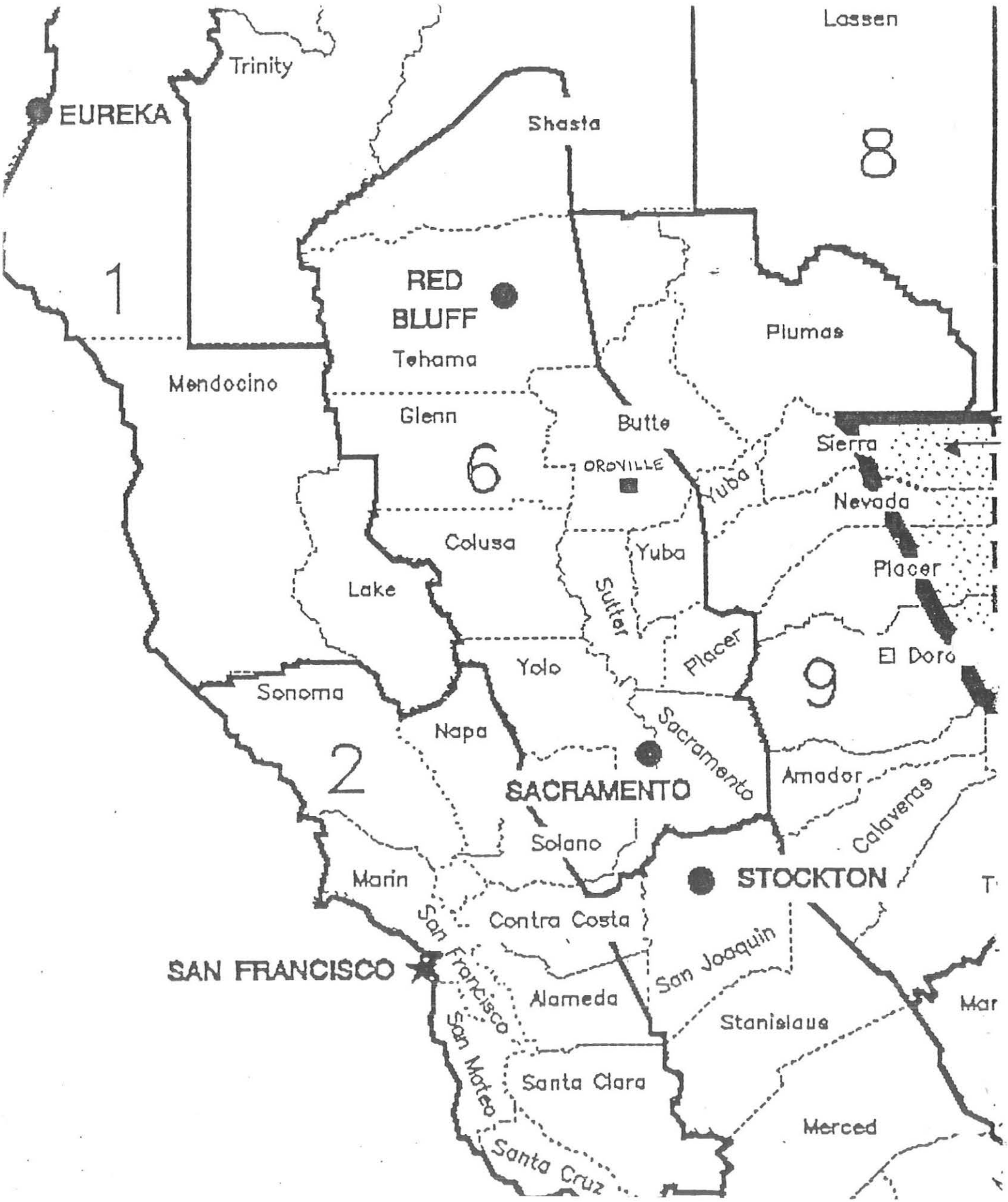

Figure 1 Map of northern California showing locations of major cities and Counties. The city of Oroville is indicated by the square in Butte County.

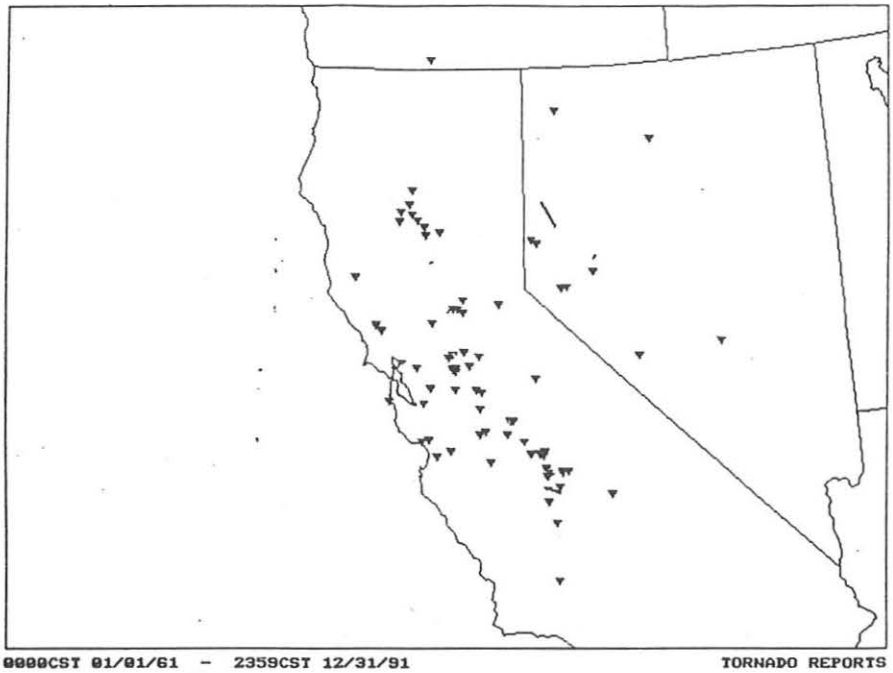

Figure 2 Tornado occurrence in northern and central California from 1961-1991. (Compiled by Storm Data)

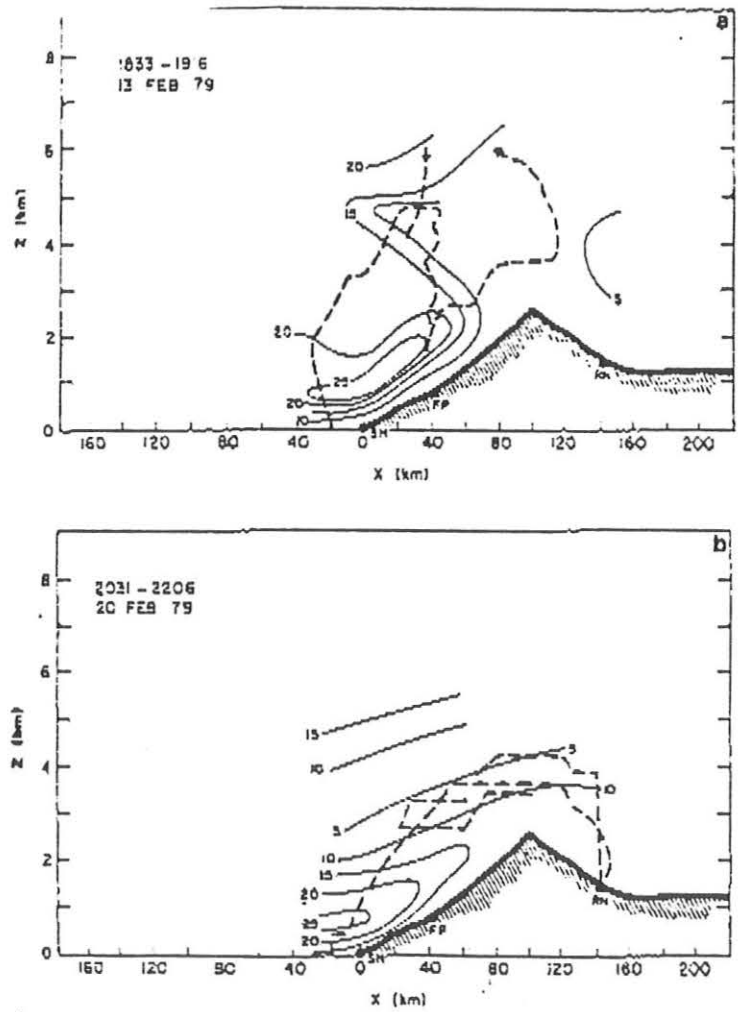

Figure 3 Mountain-parallel motion components (m s^{-1}) derived from rawinsonde and K/A data for 13 and 21 February 1979. Flight track shown by dashed line; flight time listed at top. (From Parish, 1982)

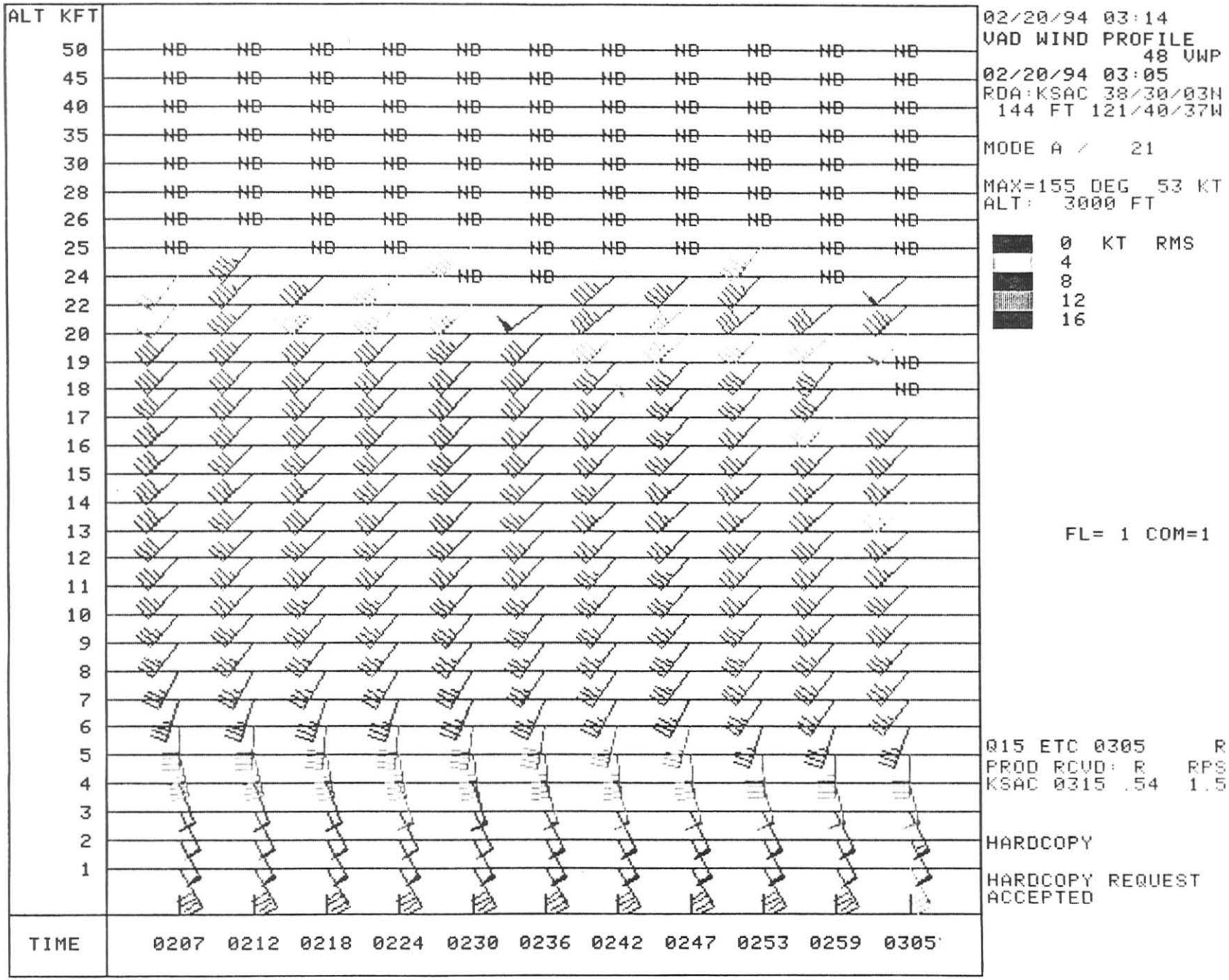

Figure 4 VAD wind profiler data from Sacramento WSR-88D for 20 February 1994. Note strong winds in the lowest 3000 feet.

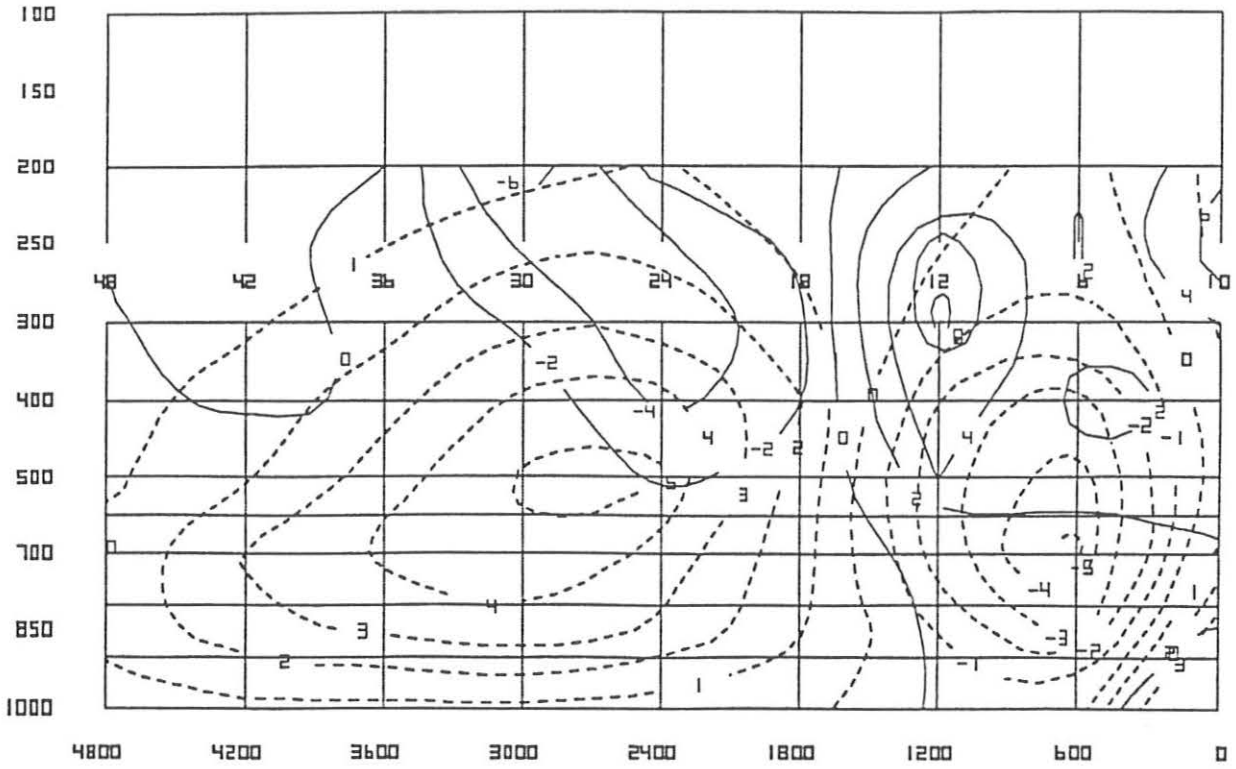

Figure 5 Time-height cross-section of vorticity advection contoured every $1x10^{-10}s^{-2}$ (solid) and vertical velocity contoured every contoured every $1\mu b\ s^{-1}$ (dashed) for 40°N 122°W.

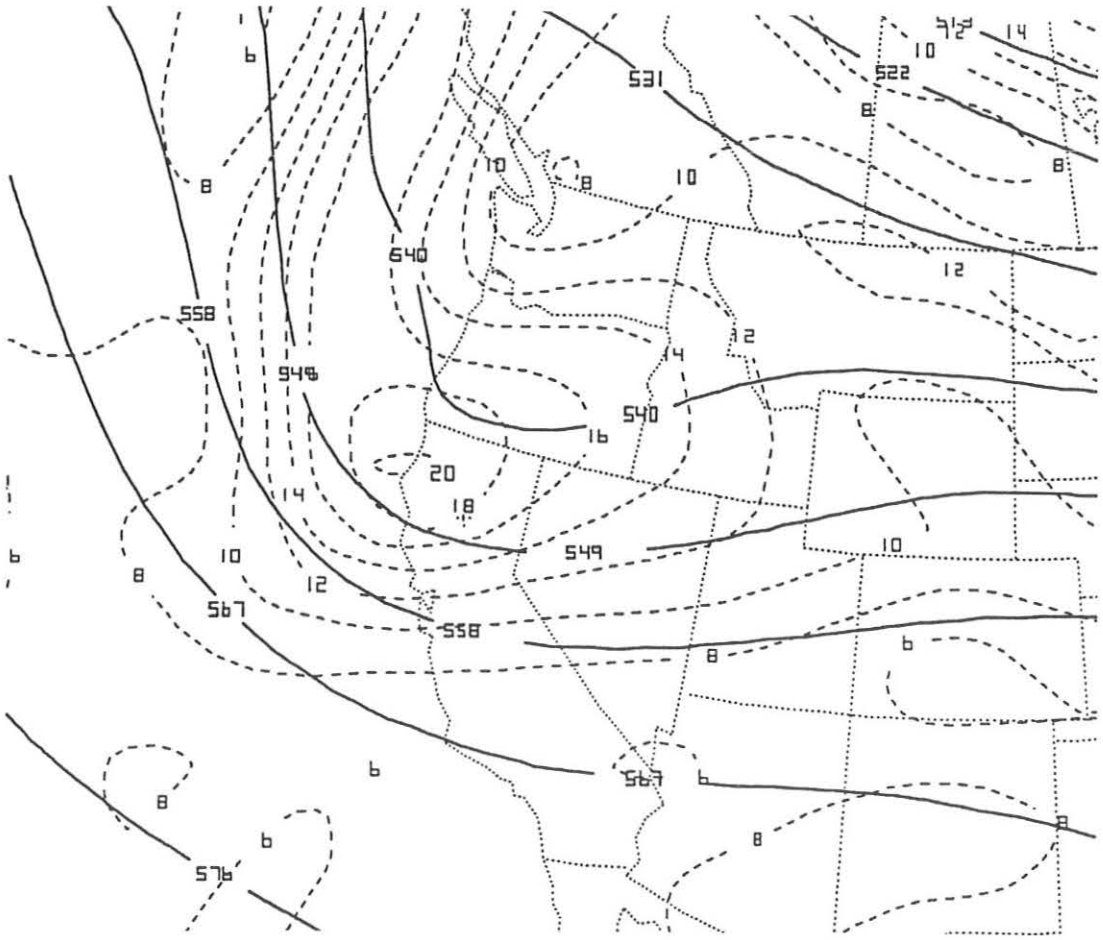

Figure 6 Height contoured every 6 dam (solid) and vorticity contoured every $2x10^{-5}\ s^{-1}$ (dashed) at 500 mb valid 0000 UTC 11 February 1994.

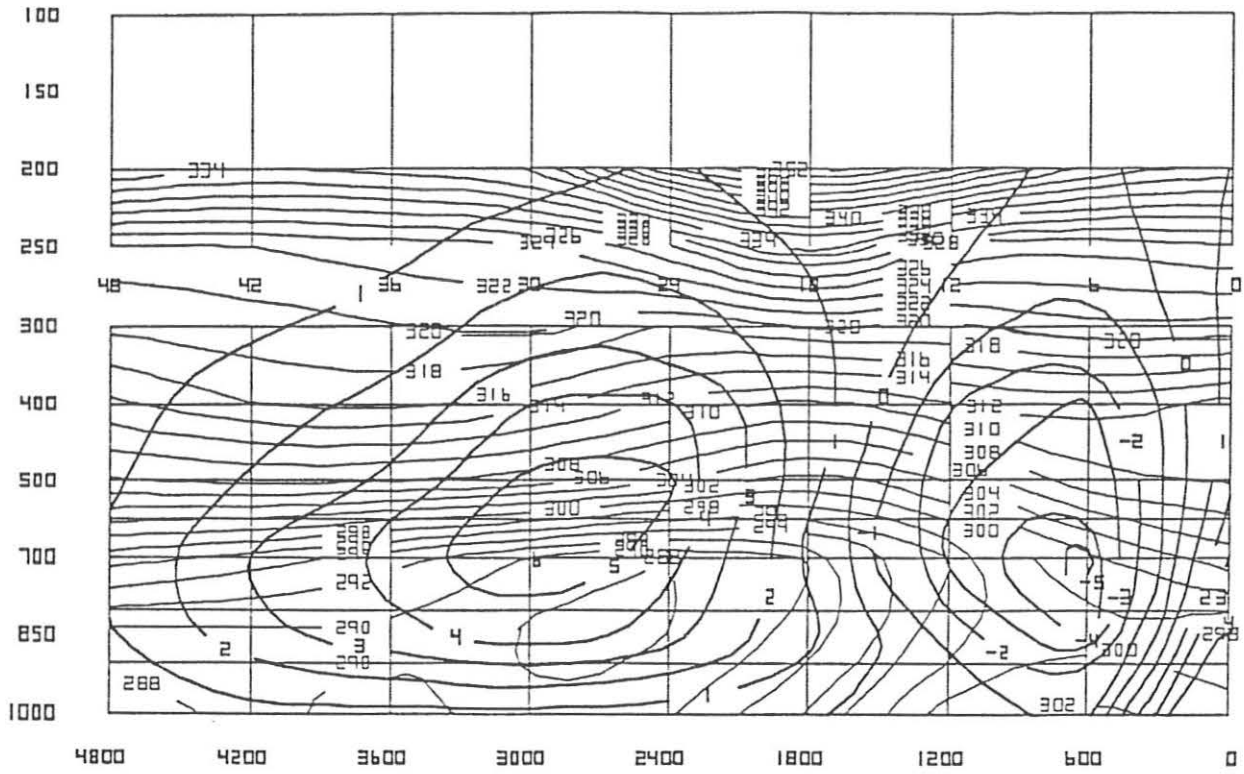

Figure 7 Time-height cross-section of equivalent potential temperature (K) (solid) and vertical velocity contoured every 1μb s^{-1}.

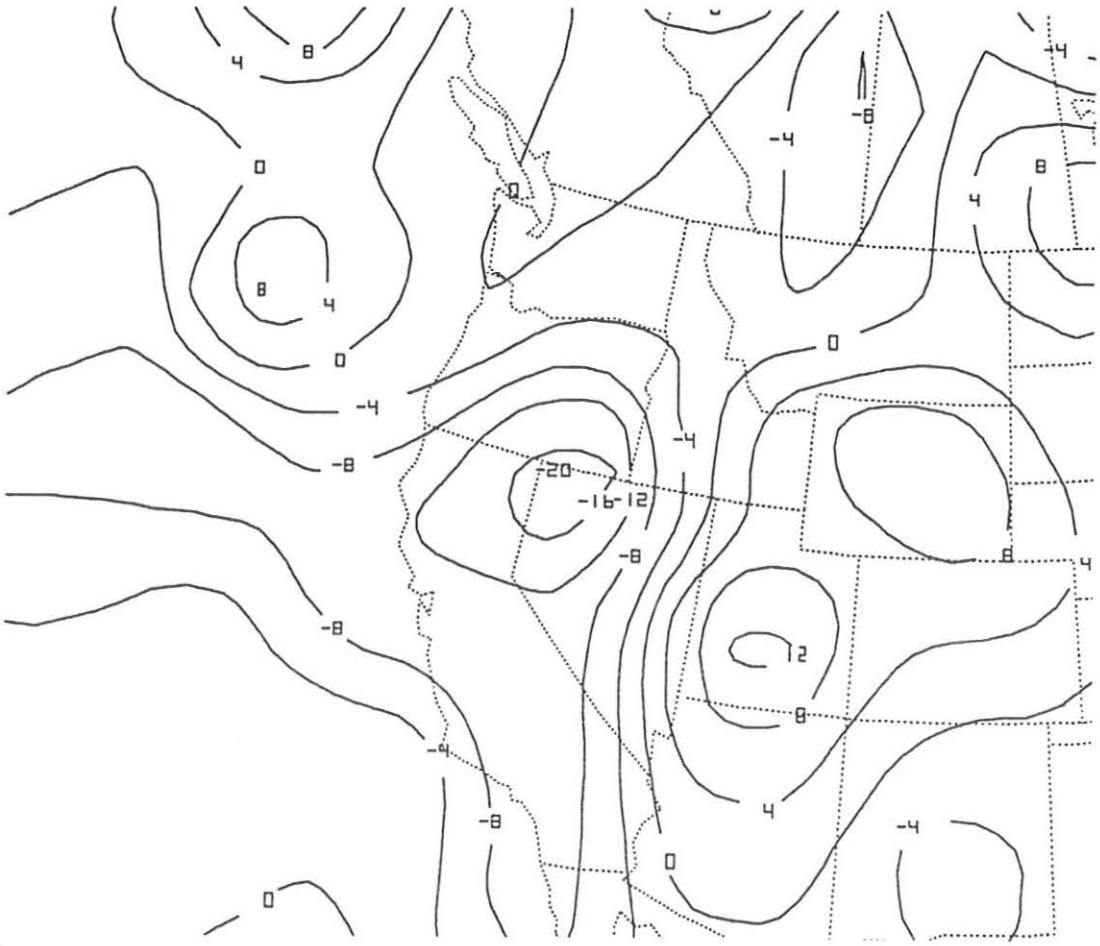

Figure 8 Temperature advection contoured every $2x10^{-4}$ °C s^{-1} in the 1000-500 mb layer valid 0000 UTC 11 February 1994.

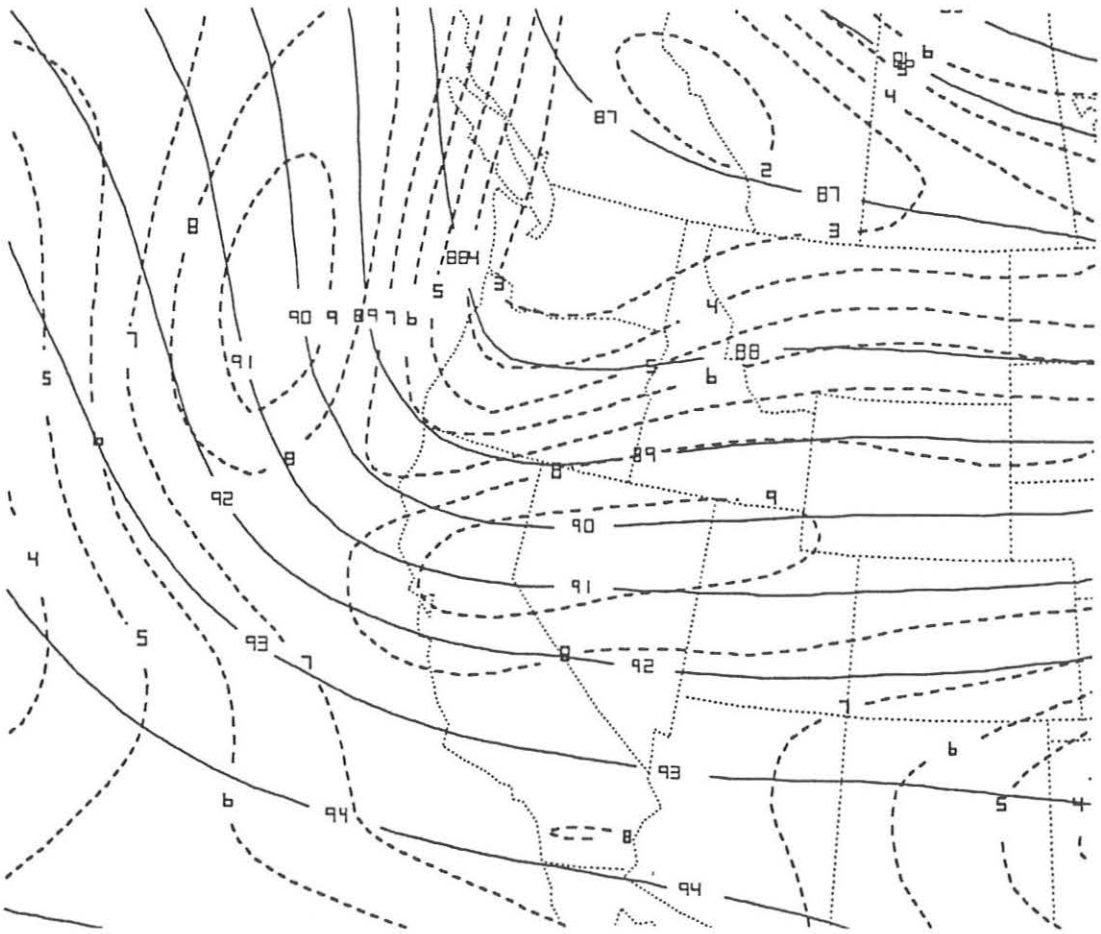

Figure 9 Height (solid) contoured every 12 dam and wind speed contoured every 10 knots (dashed) at 300 mb valid 1200 UTC 10 February 1994.

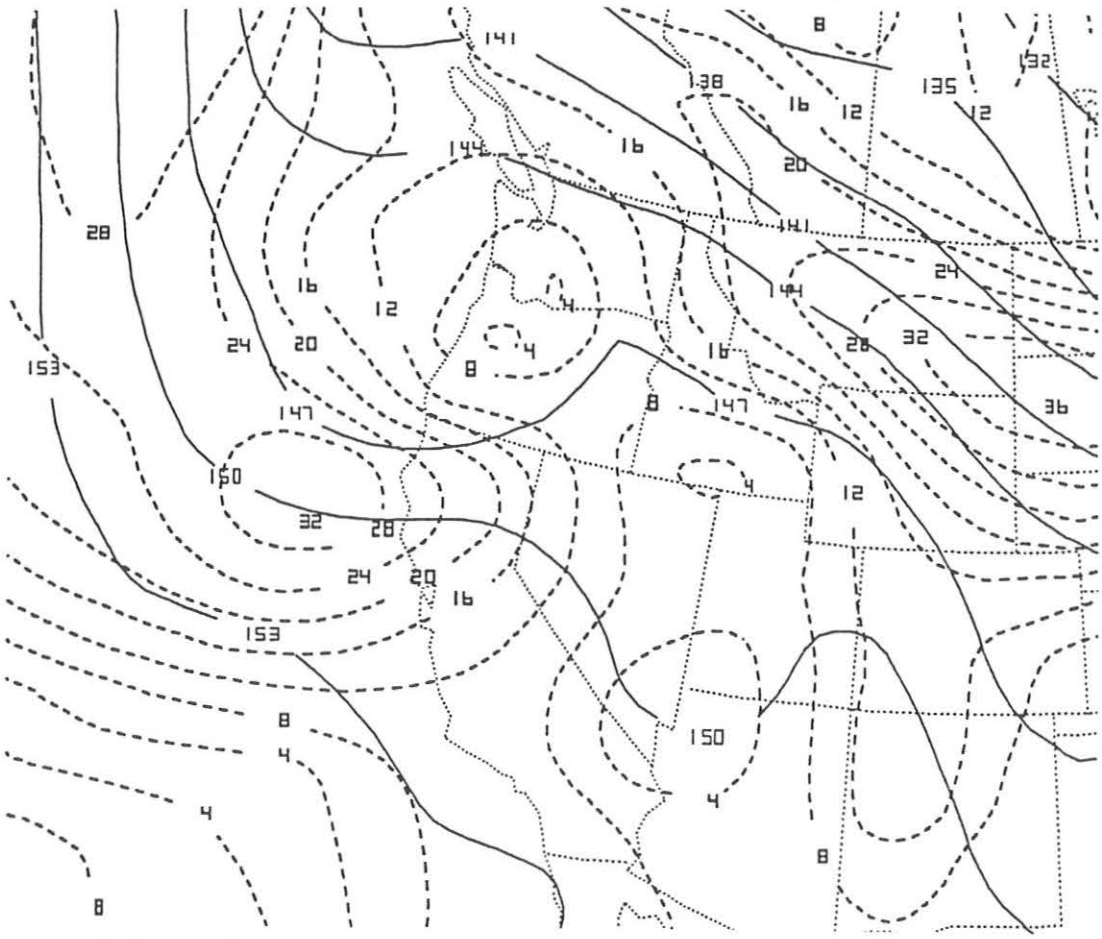

Figure 10 Height (solid) contoured every 3 dam and wind speed contoured every 10 knots (dashed) at 850 mb valid 0000 UTC 10 February 1994.

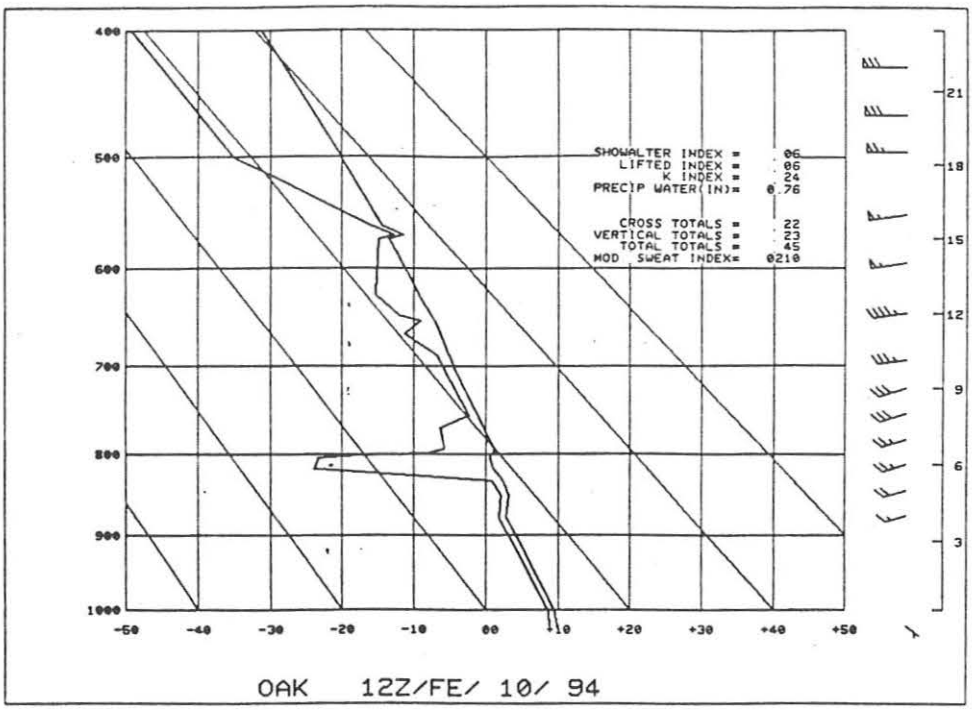

Figure 11 The Oakland (OAK) sounding for 1200 UTC 10 February 1994.

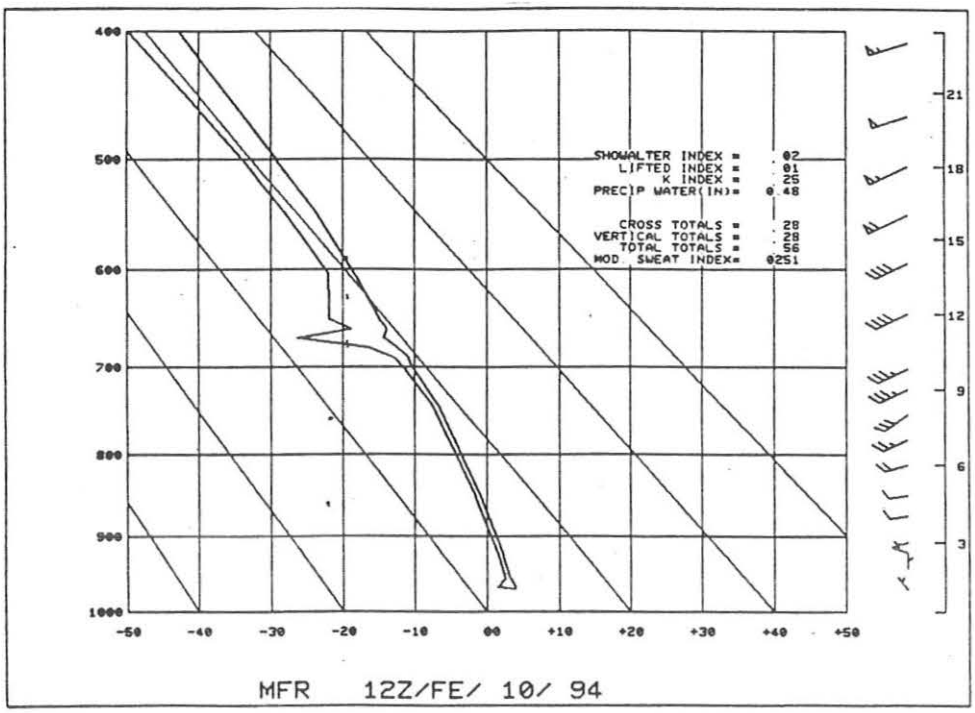

Figure 12 The Medford (MFR) sounding for 1200 UTC 10 February 1994.

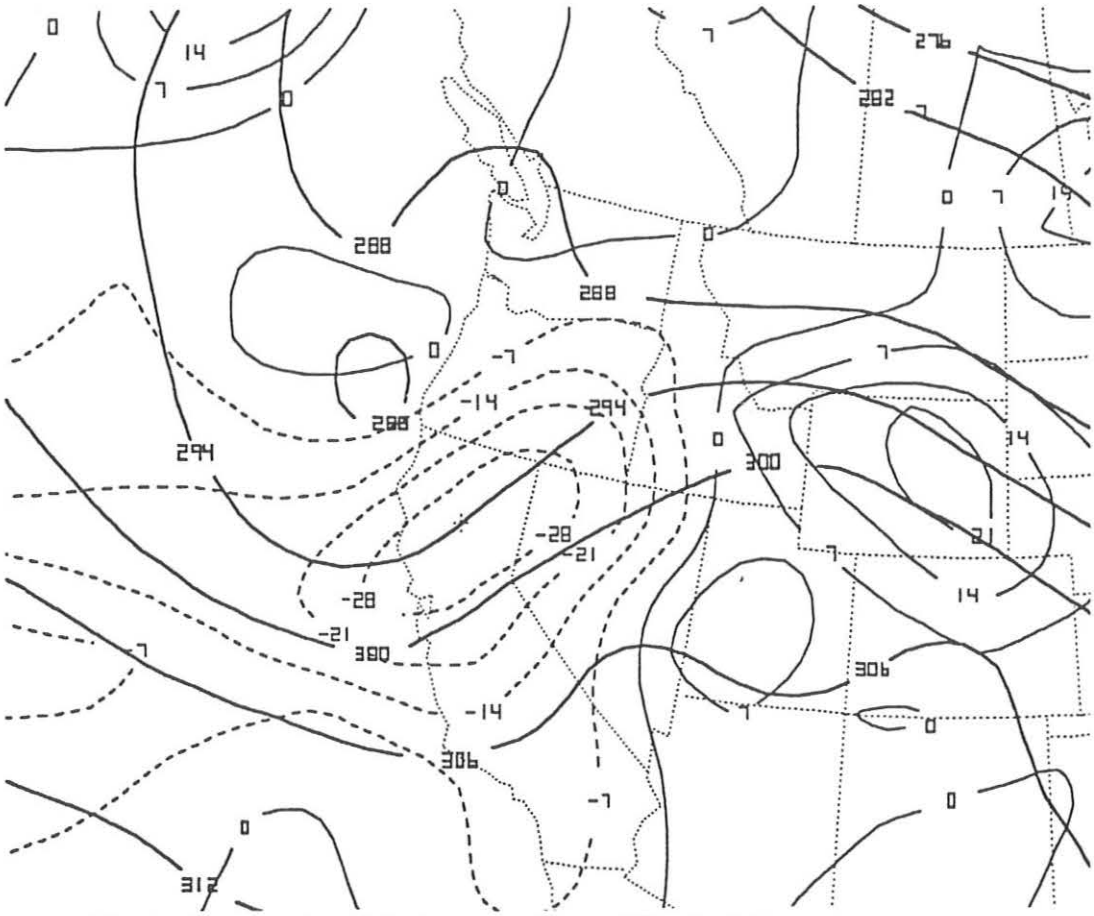

Figure 13 Equivalent potential temperature (K) (solid) and equivalent potential temperature (K) advection contoured every 0.7 K s^{-1} (dashed) at 700 mb valid 0000 UTC 11 February 1994.

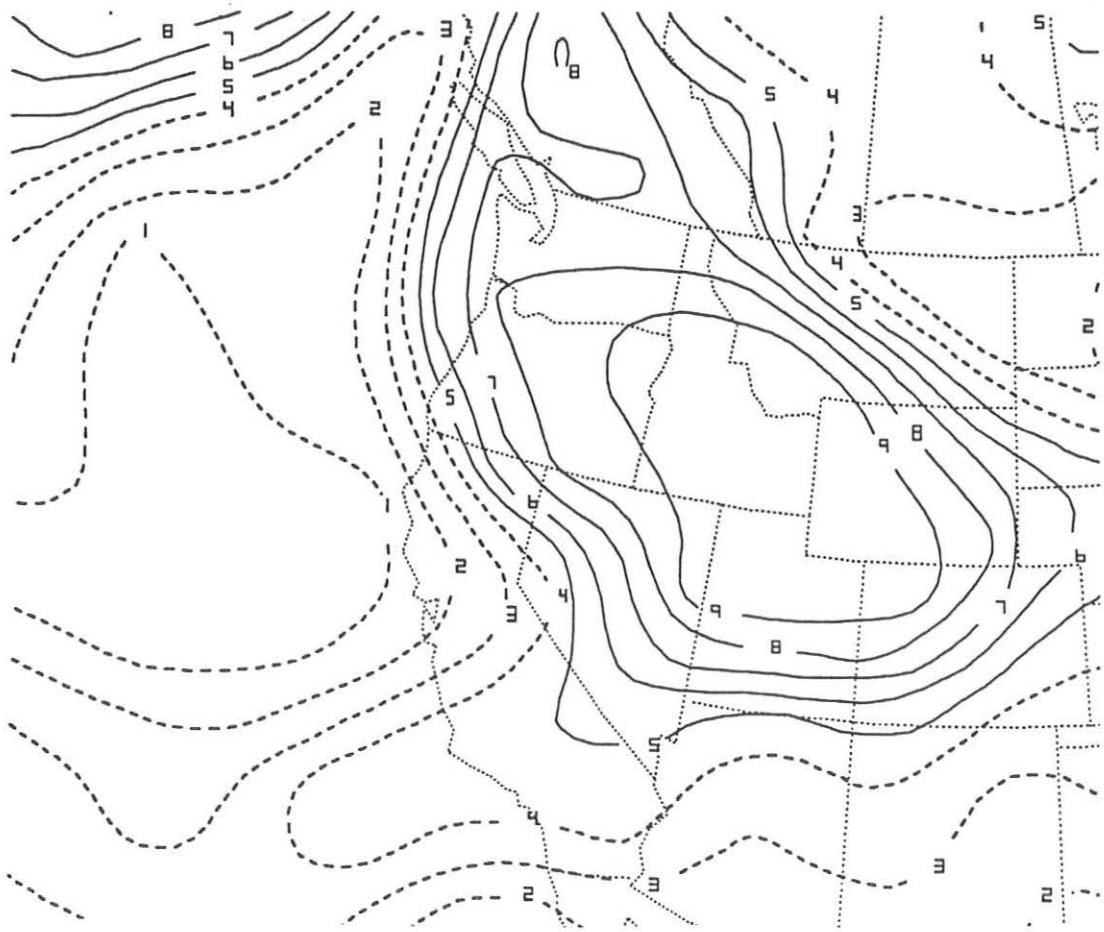

Figure 14 Relative humidity (in 10 percent intervals) at 500 mb valid 0000 UTC 11 February 1994.

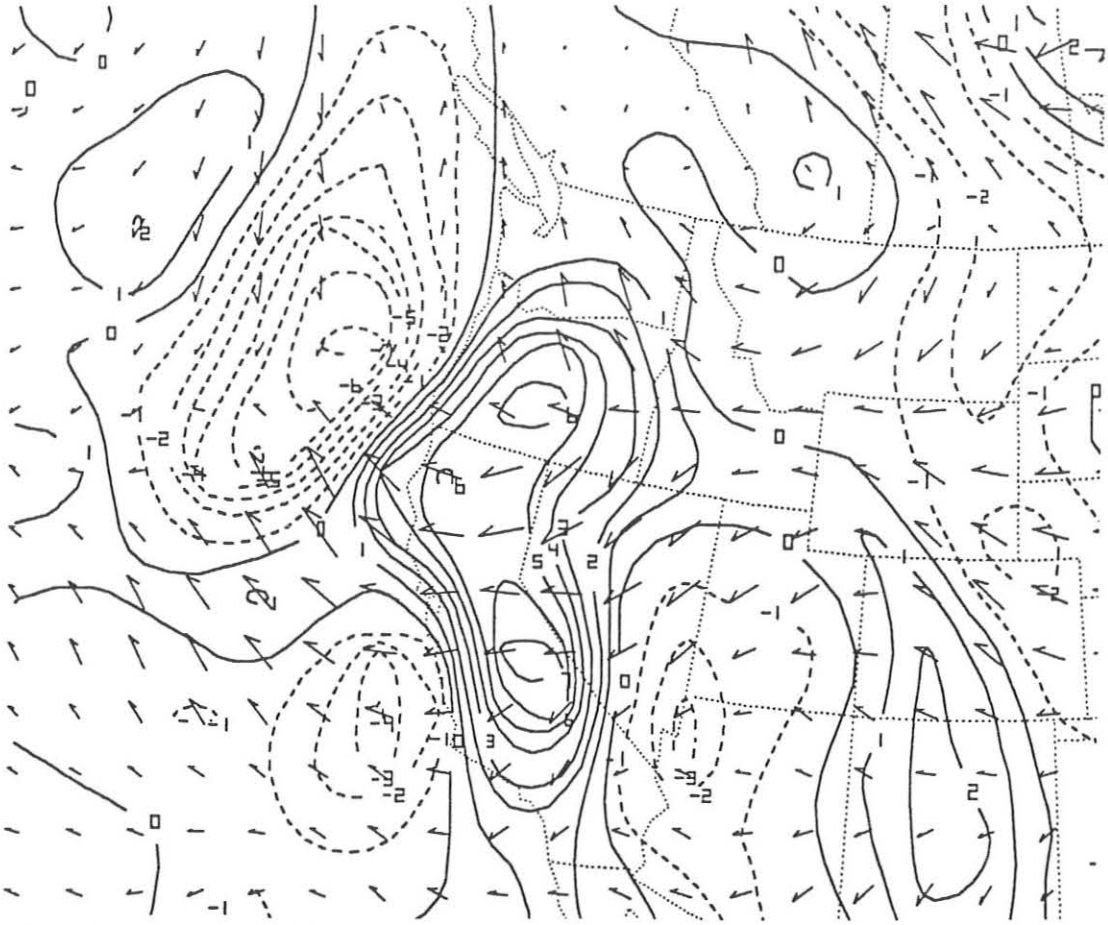

Figure 15 Q-vectors and Q-vector convergence (solid) in the 850-400 mb layer valid 0000 UTC 11 February 1994.

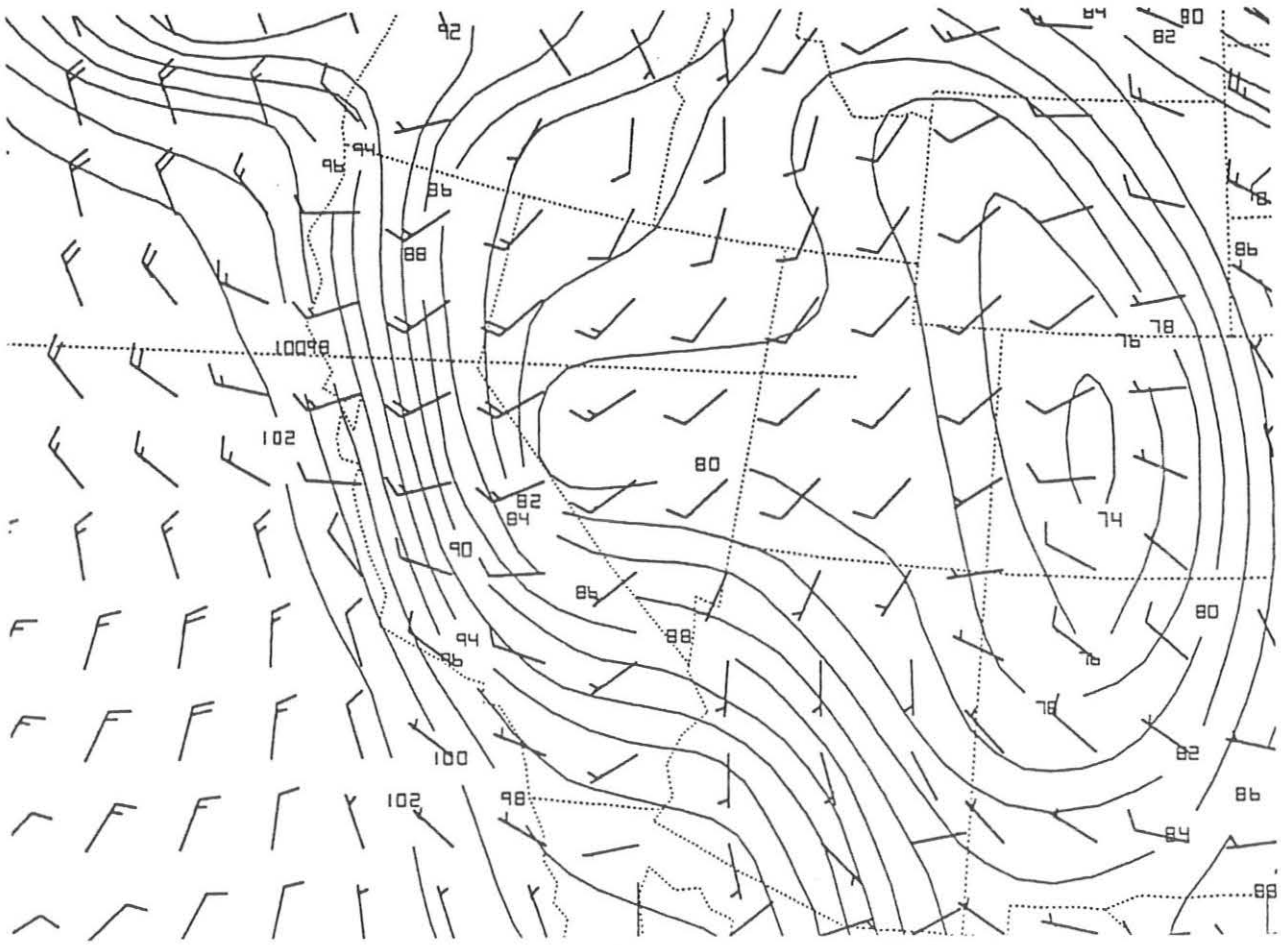

Figure 16 280K isentropic surface with pressure, contoured every 20 mb, (solid) and wind barbs valid 1800 UTC 10 February 1994.

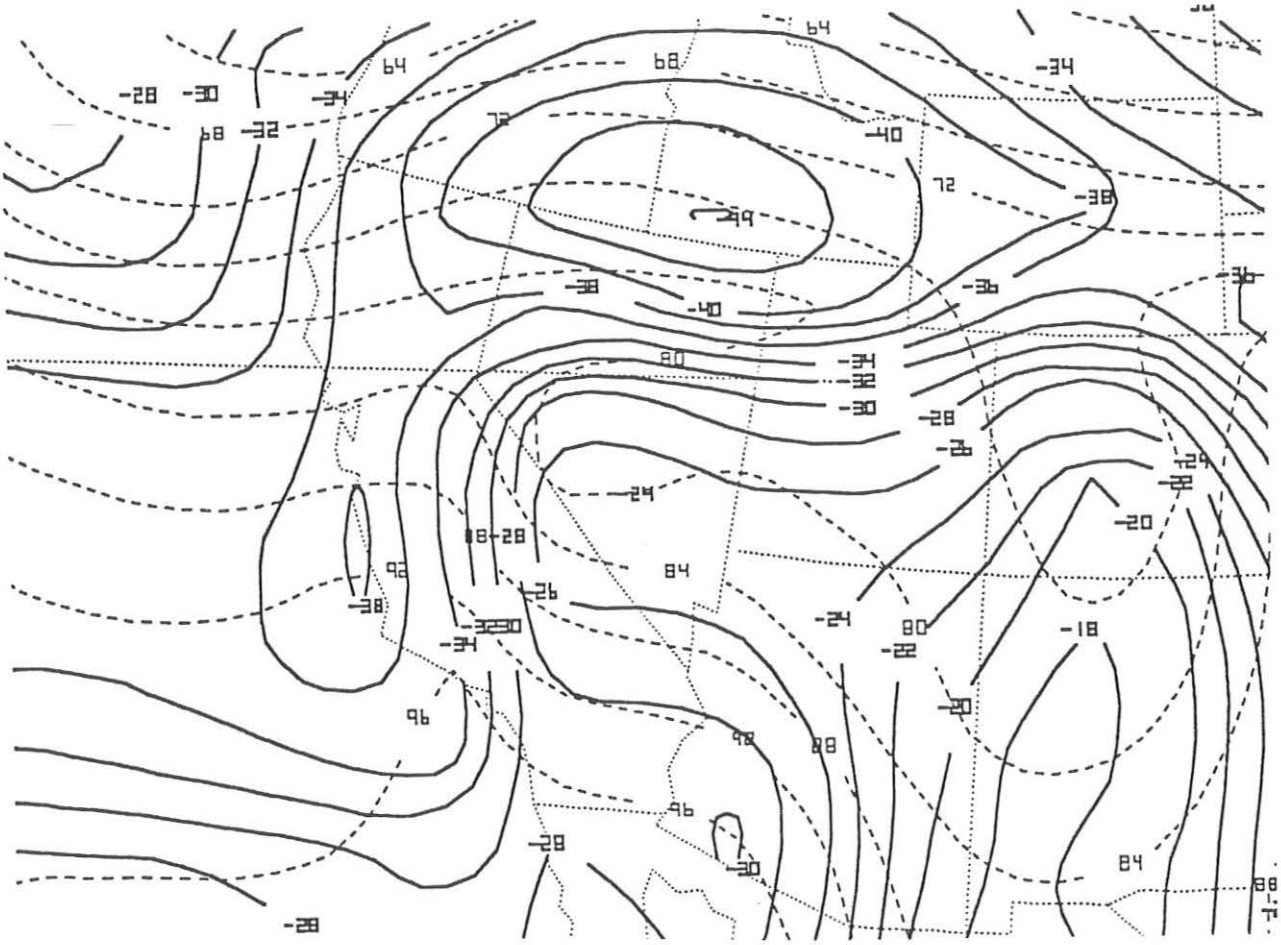

Figure 17 286-306K isentropic layer with stability (dark solid) and pressure at 306K (dashed) valid 1800 UTC 10 February 1994.

Figure 18 Adiabatic moisture flux convergence (solid) with wind vectors valid 1800 UTC 10 February 1994.

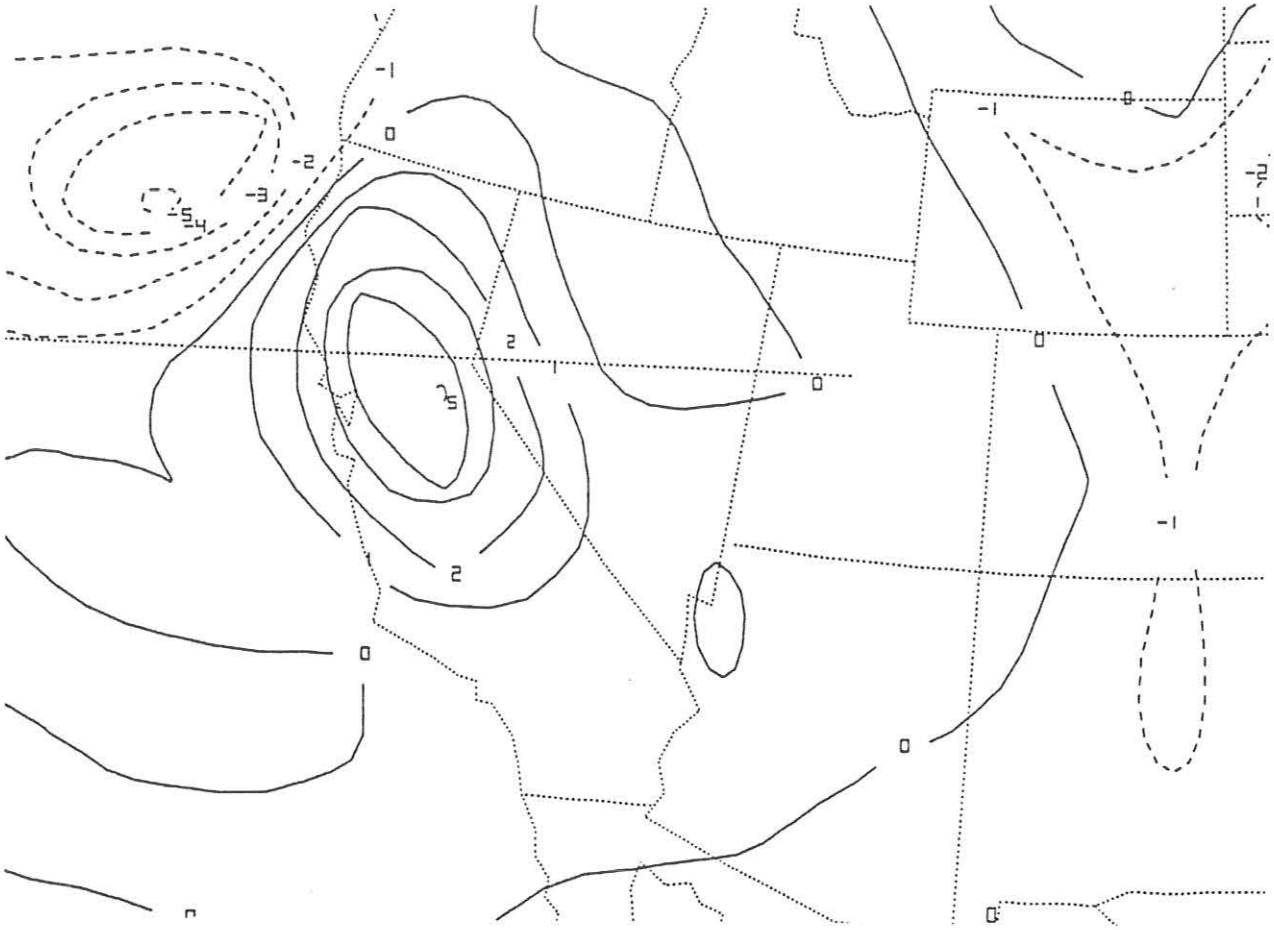

Figure 19 Vertical velocity contoured every 1μb s^{-1} due to pressure advection in the 286-306K isentropic layer valid 1800 UTC 10 February 1994.

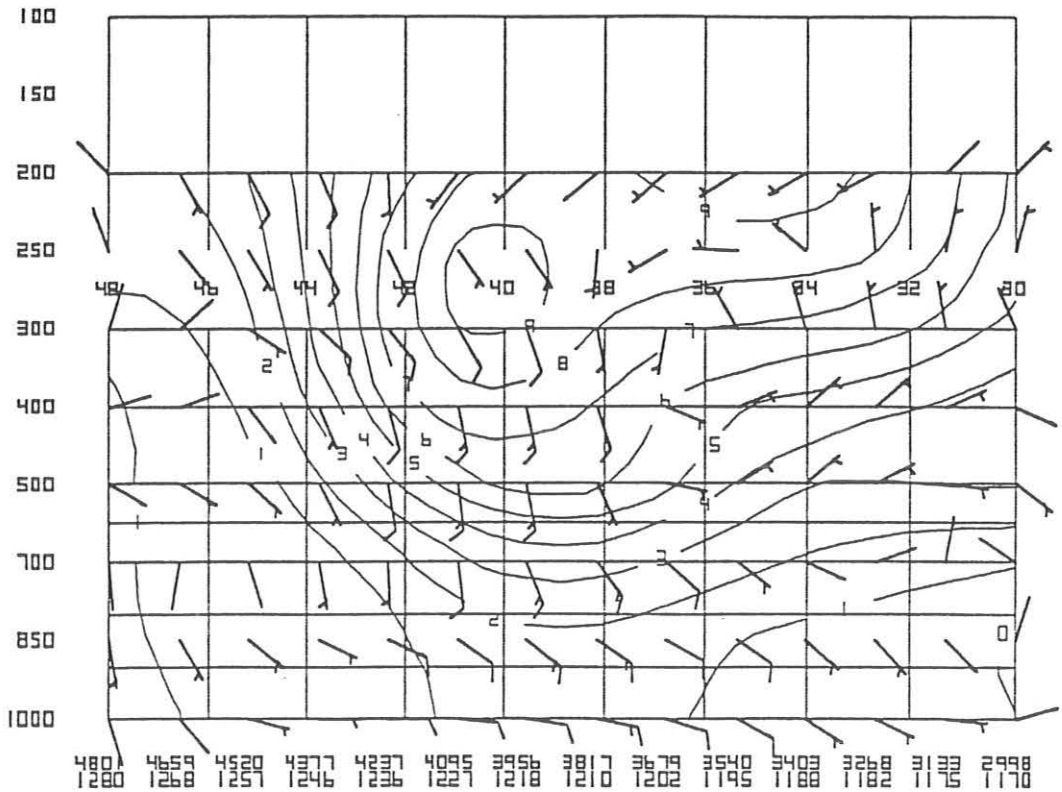

Figure 20 Cross-section from 48°N 128°W to 30°N 117°W with ageostropic wind (barbs) and normalized wind speed contoured every 10 knots (solid) valid 1800 UTC 10 February 1994.

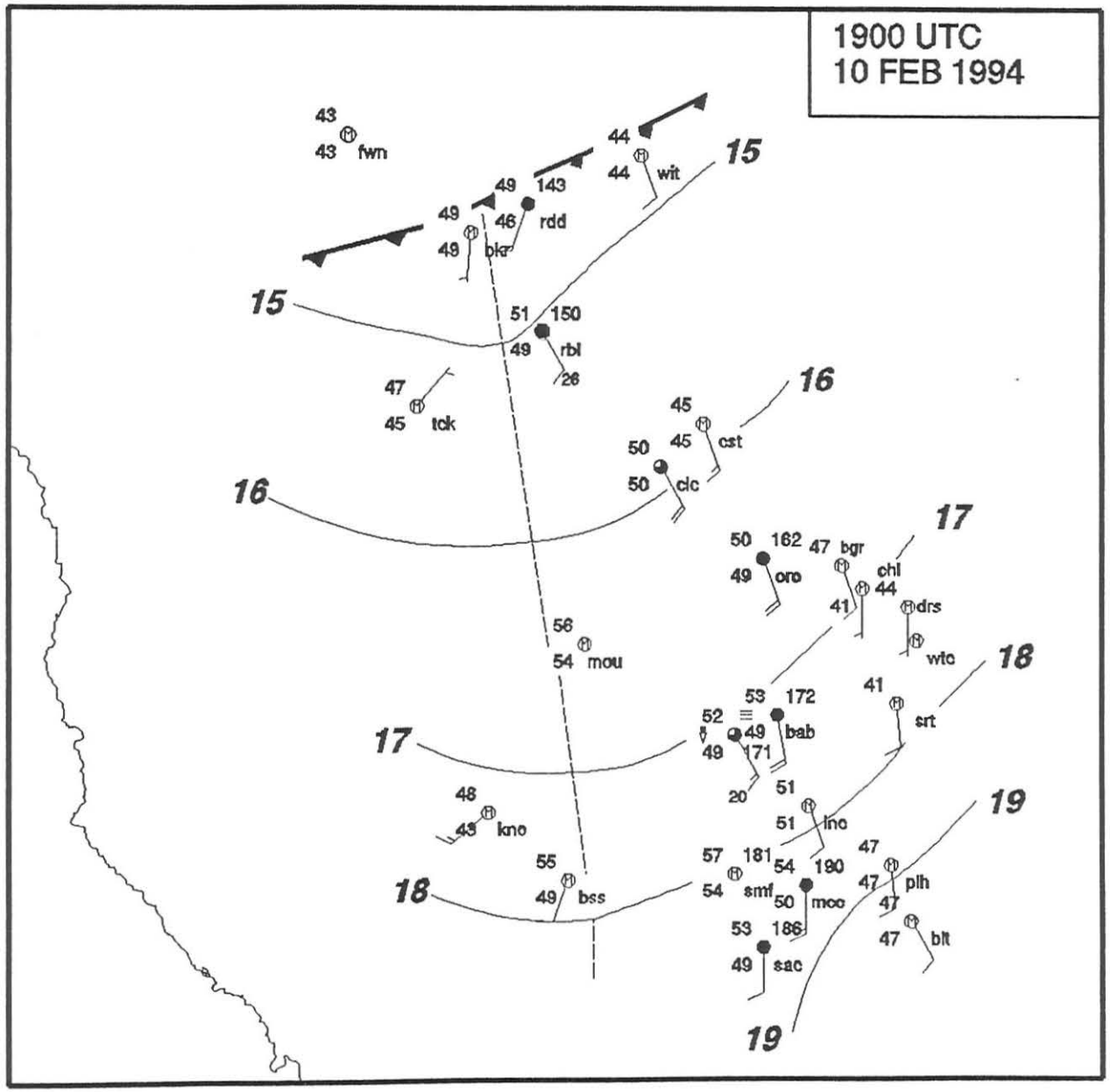

Figure 21 1900 UTC 10 February sub-synoptic pressure analysis (solid lines, every mb) indicating weak pressure trough (dashed line) along with a windshift/moisture discontinuity (solid front with barbs).

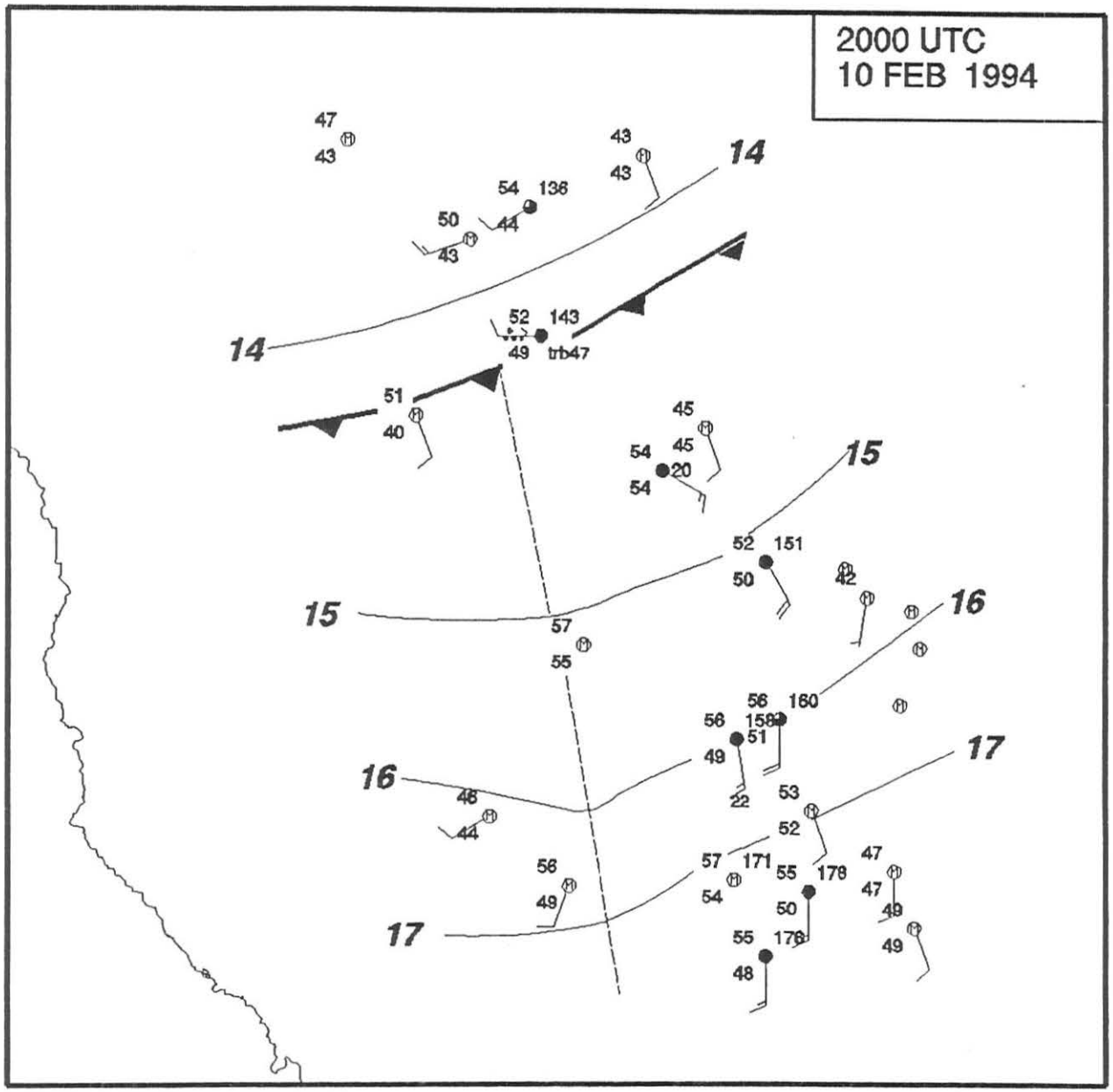

Figure 22 Same as Figure 21 except 2000 UTC 10 February 1994.

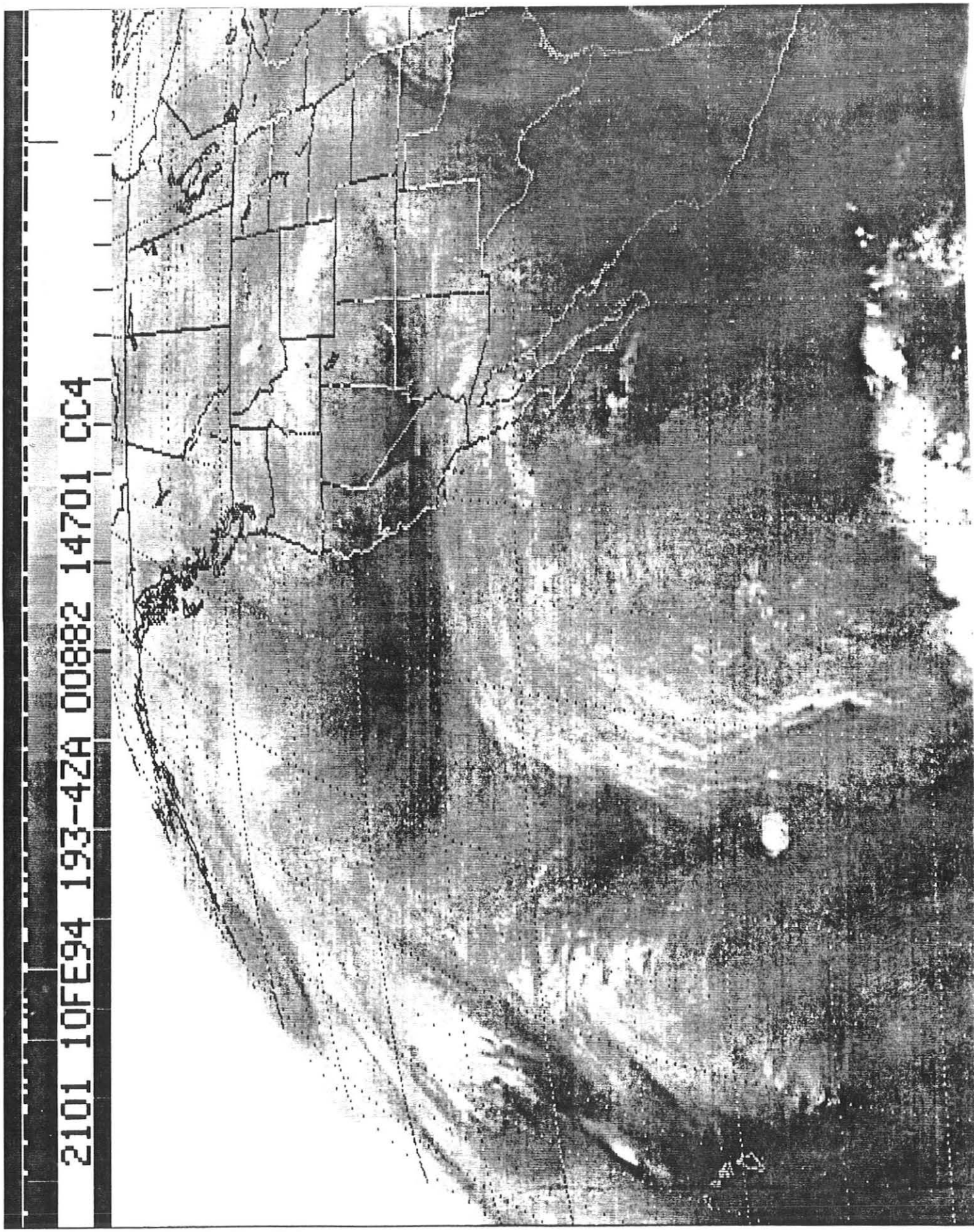

Figure 23 Water vapor imagery for 2100 UTC 10 February 1994.

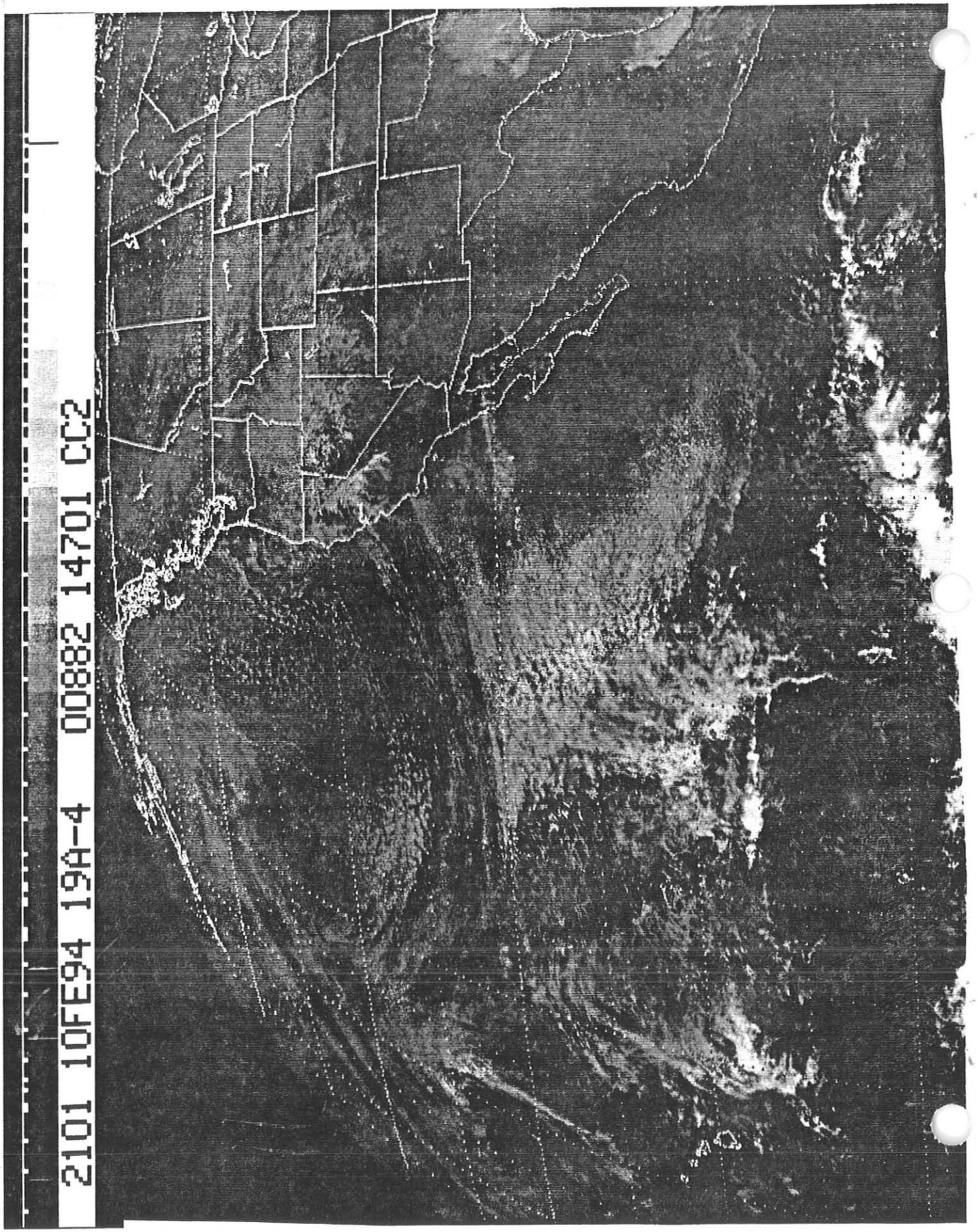

Figure 24 Visible satellite imagery for 2100 UTC 10 February 1994.

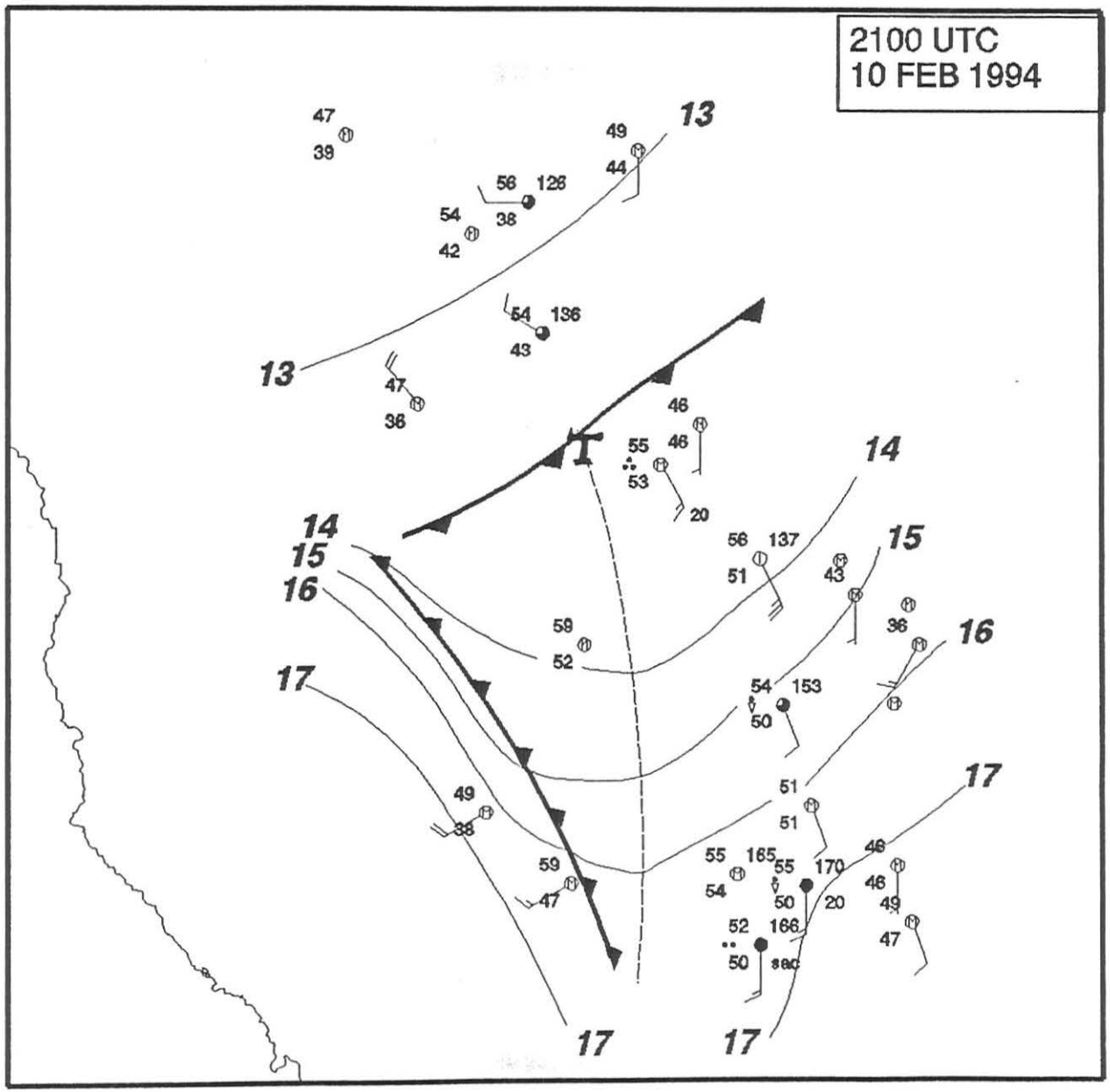

Figure 25 Same as Figure 21 except 2100 UTC 10 February 1994. Triple point indicated by T.

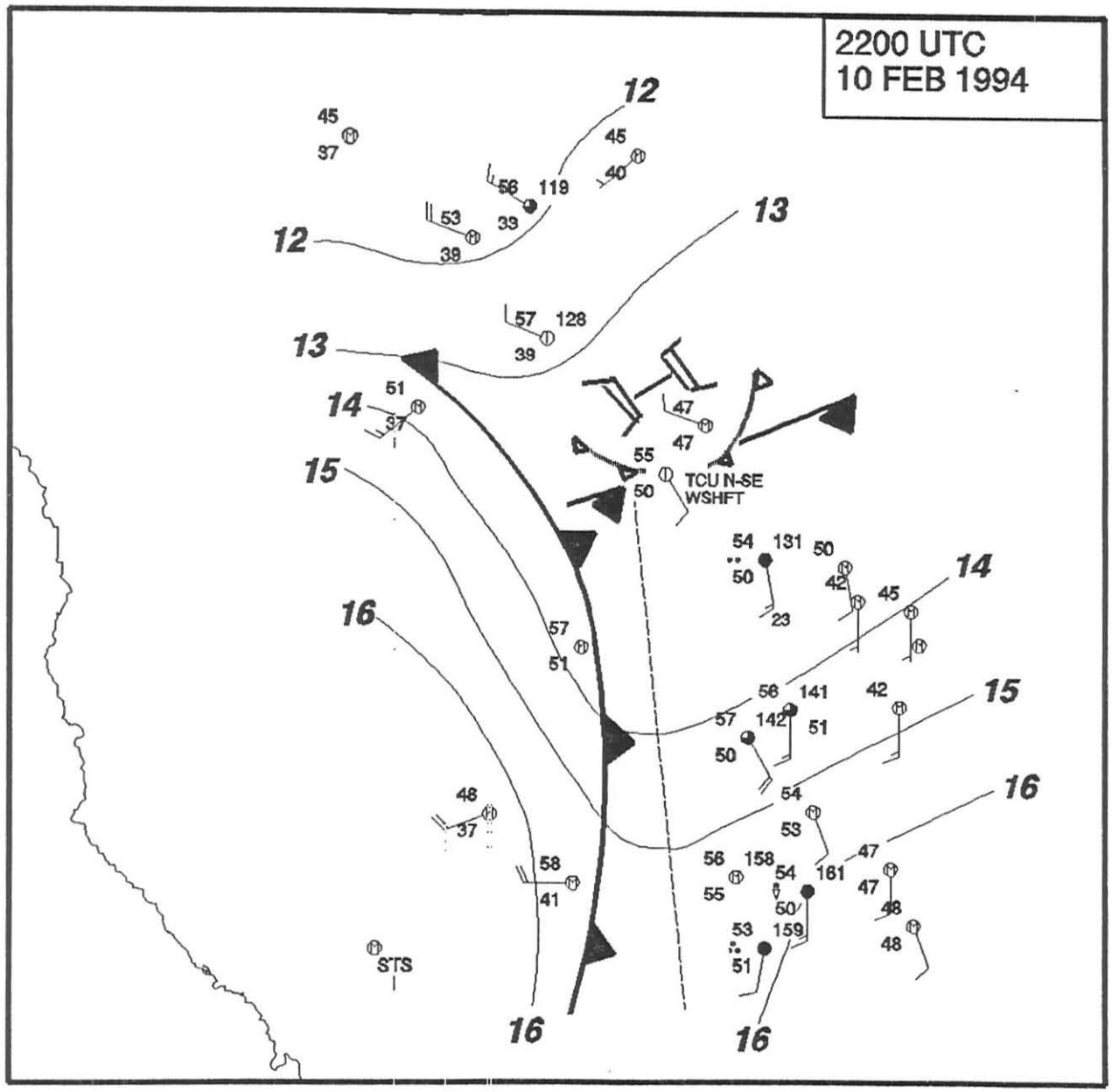

Figure 26 Same as Figure 21 except 2200 UTC 10 February 1994. Mesohigh is represented by H and outflow boundary by hatched frontal boundary.

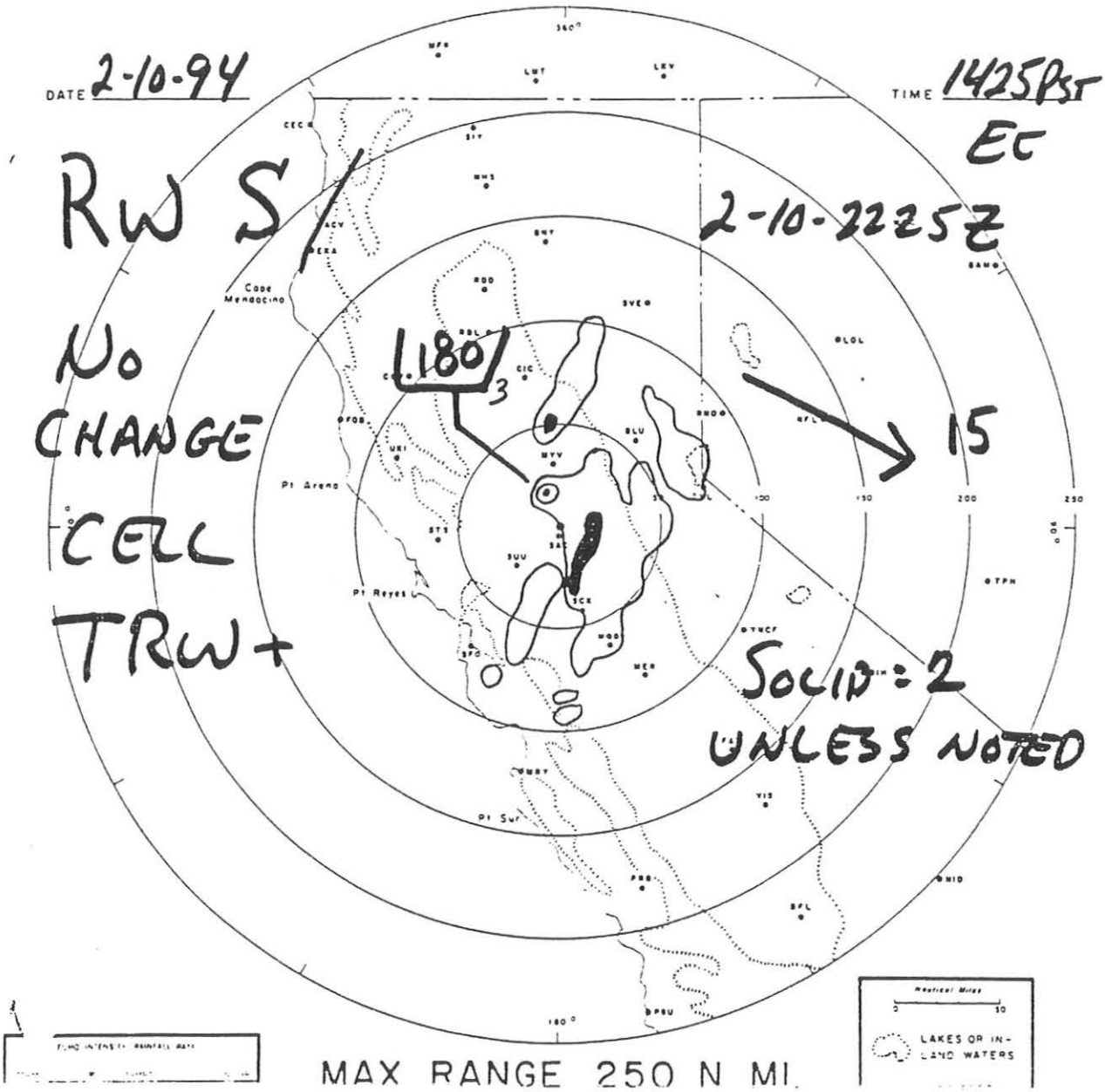

Figure 27 Sacramento WSR-57 radar overlay of precipitation echoes from 2225 UTC 10 February 1994.

Figure 28 WSR-88D 2.4° base velocity scan at 2244 UTC indicating storm top divergence. Green represents movement towards the radar and brown represents movement away.

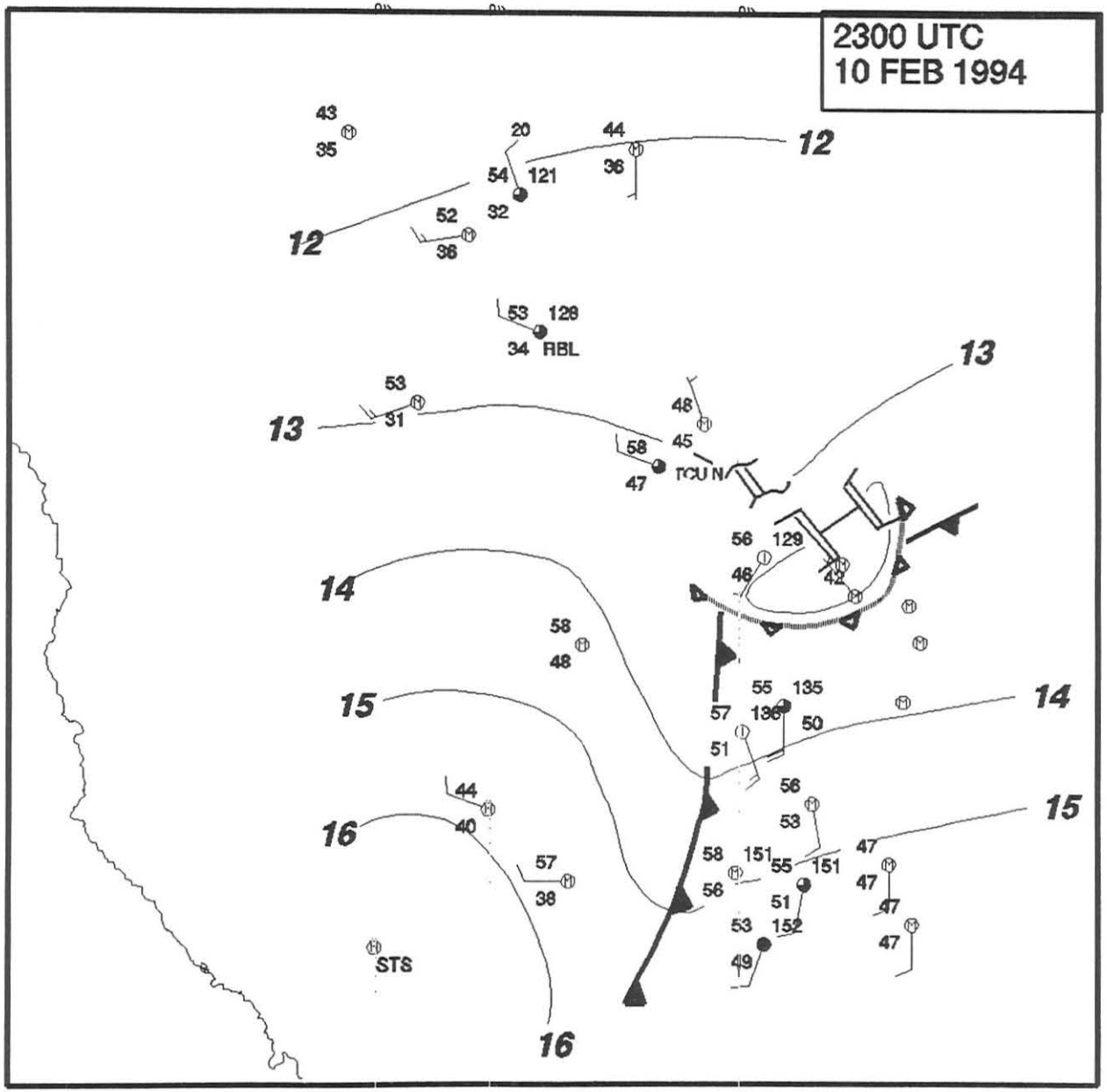

Figure 29 Same as Figure 26 except 2300 UTC 10 February 1994.

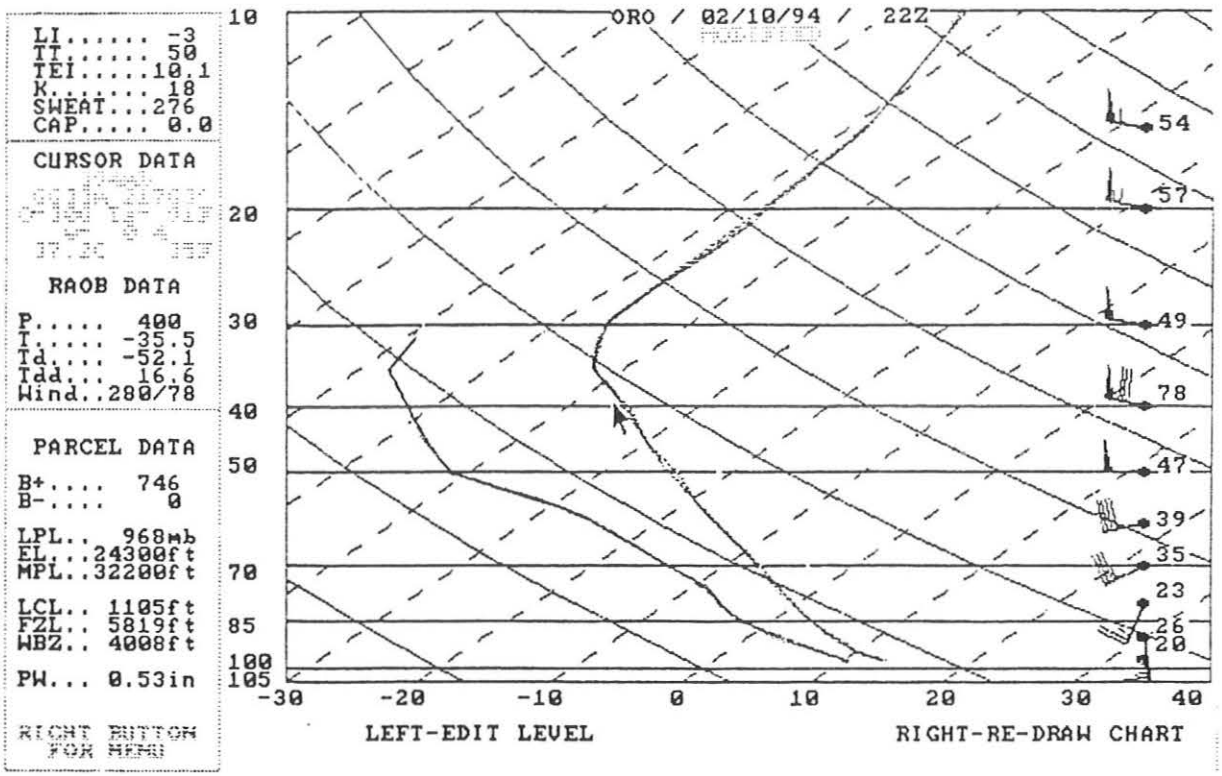

Figure 30 Modified sounding for Oroville for 2200 UTC 10 February 1994.

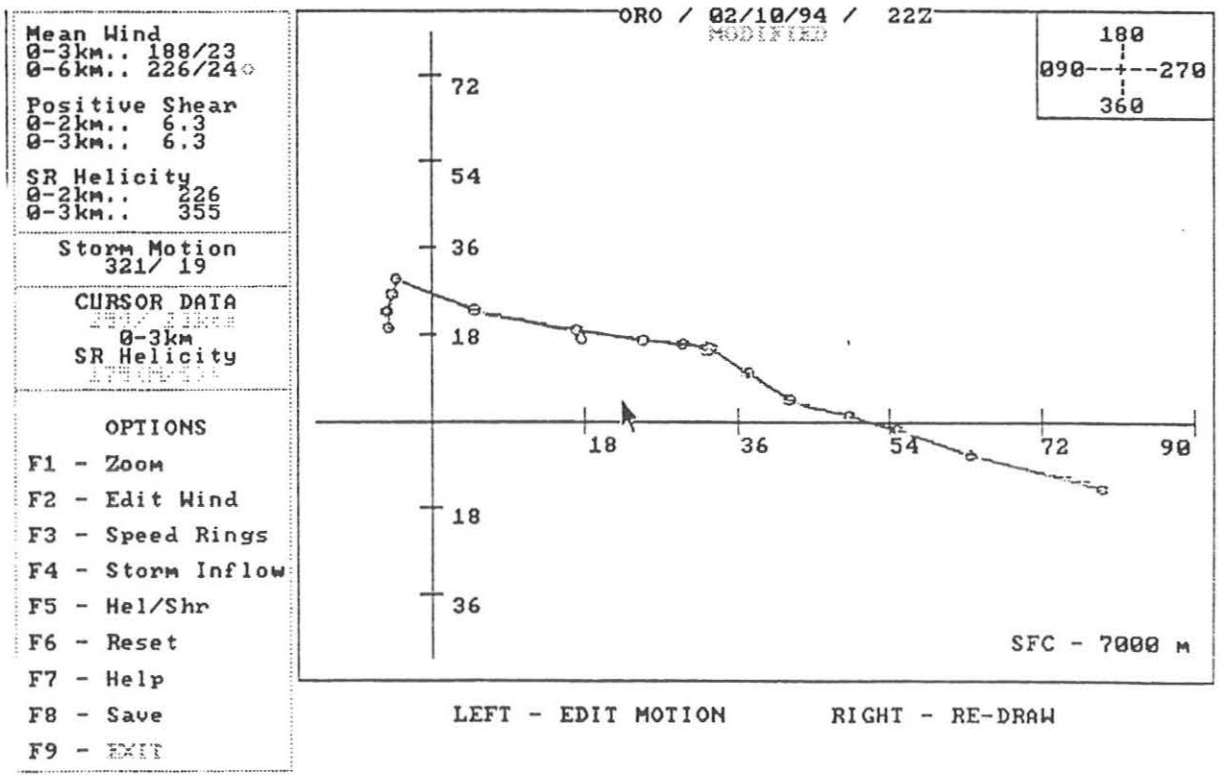

Figure 31 Modified hodograph for Oroville for 2200 UTC 10 February 1994.

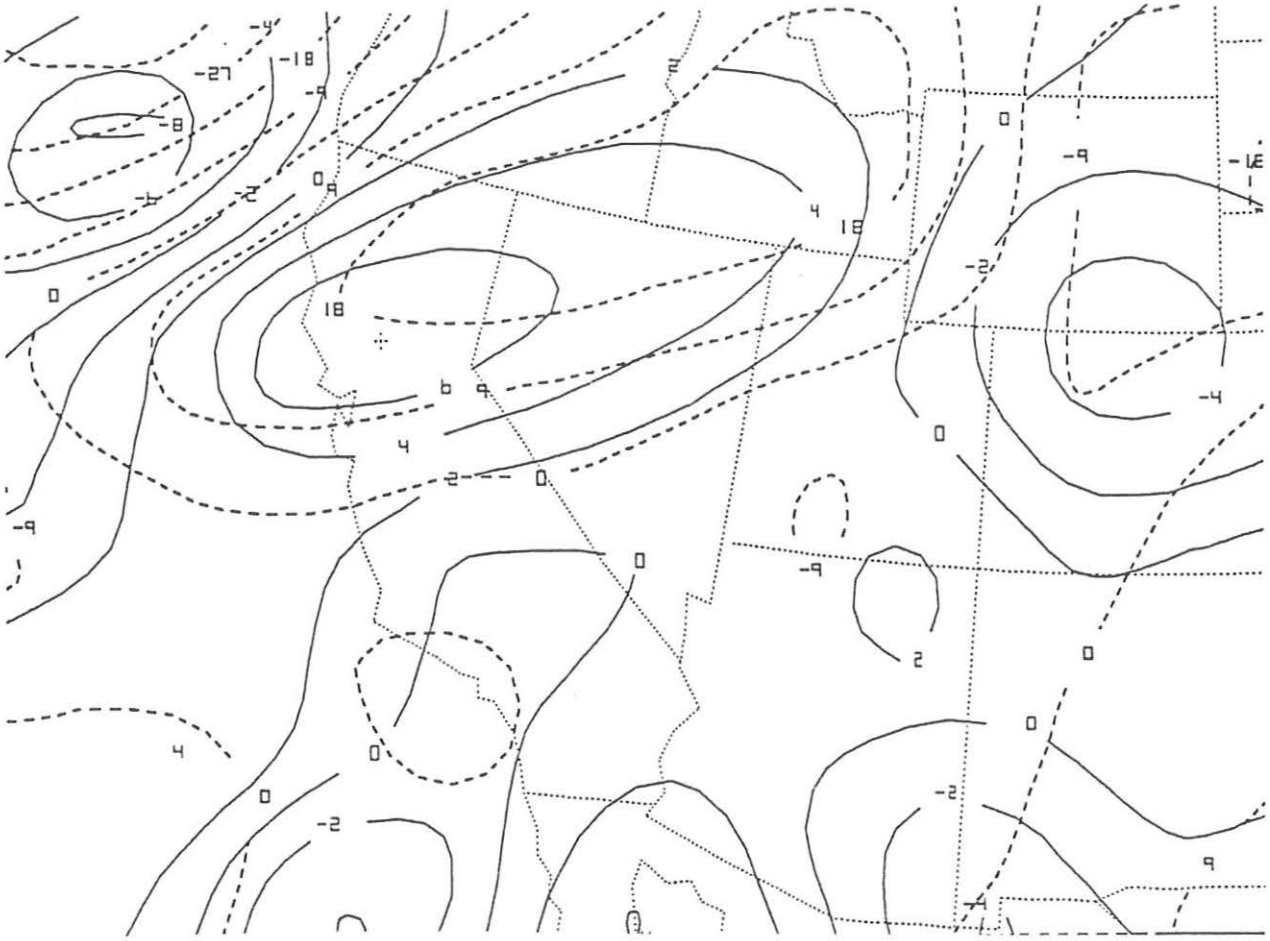

Figure 32 Warm air advection contoured every $1x10^{-4}$ °C s^{-1} (dashed) with cyclonic vorticity advection contoured every $1x10^{-10}$ s^{-2} (solid) at 250 mb valid 0000 UTC 11 February 1994.

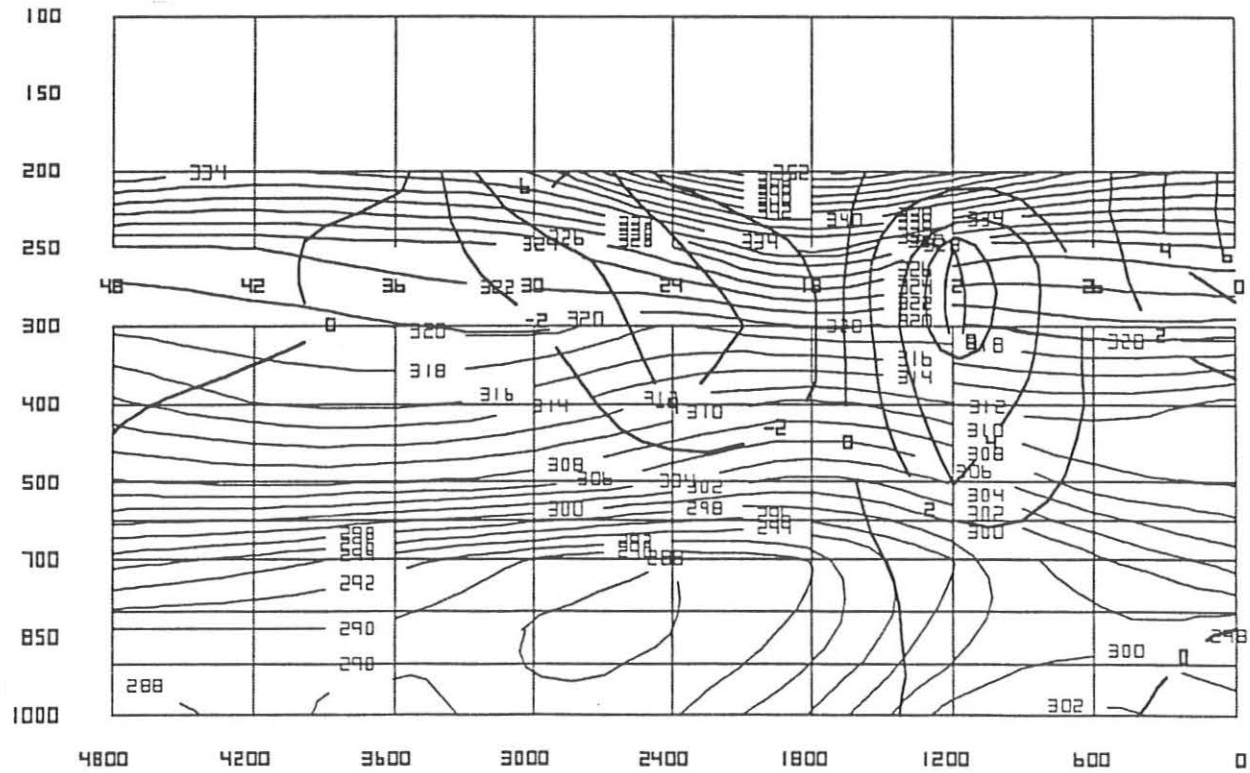

Figure 33 Time-height cross-section at 40°N 122°W with equivalent potential temperature (K) (solid) and vorticity advection (dark solid). Note strong cyclonic vorticity advection contoured every $1x10^{-10}$ s^{-2} ahead of the tropopause fold.

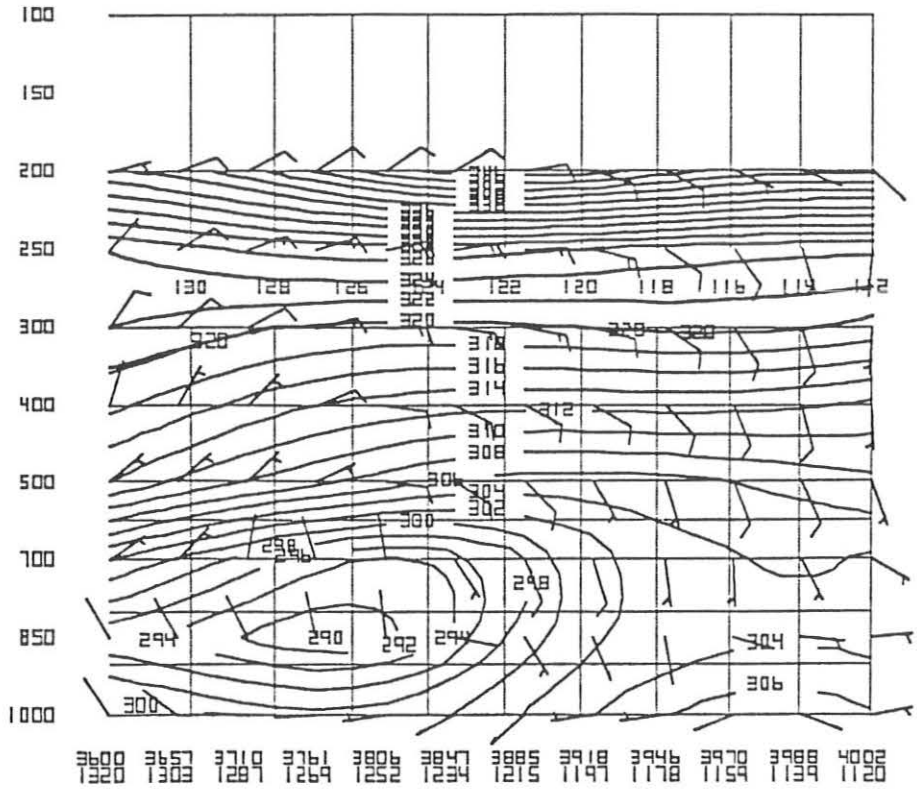

Figure 34 Cross-section from 36°N 132°W to 40°N 112°W with ageostropic circulations (barbs) and equivalent potential temperature (K) (solid) valid 0000 UTC 11 February 1994.

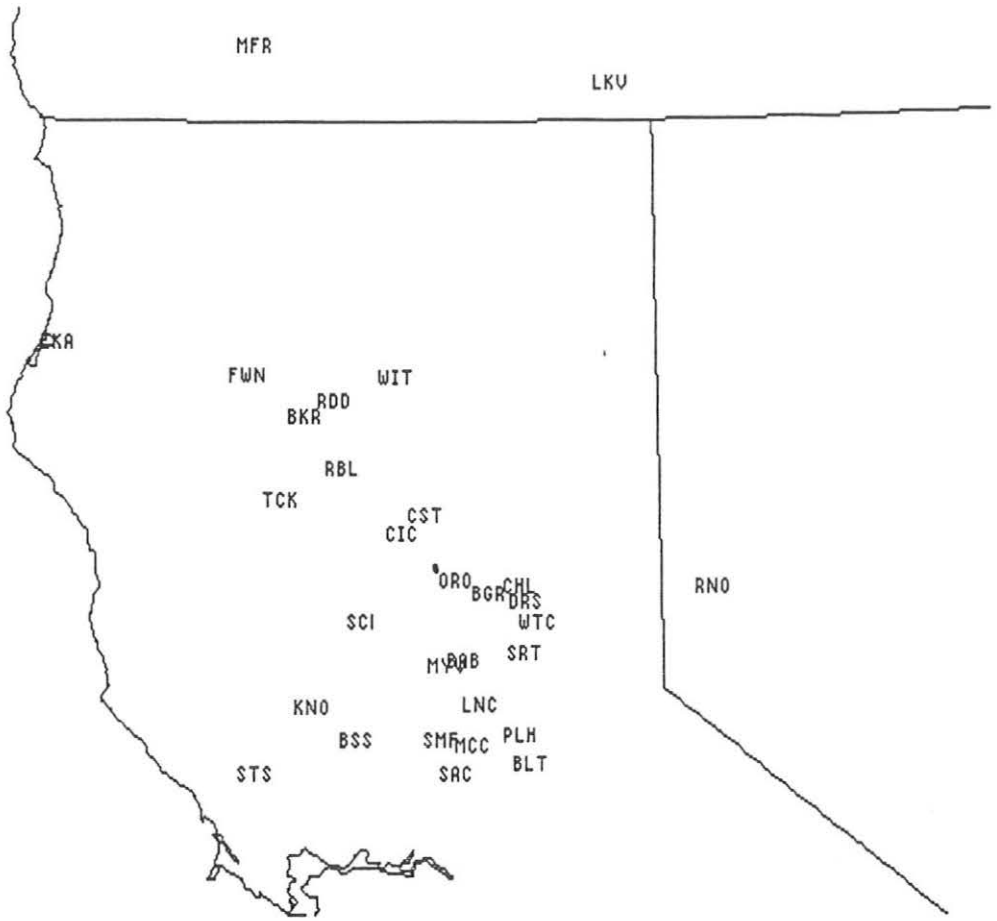

Appendix A Map of northern California with three-letter identifiers. Oroville is ORO.

142 The Usefulness of Data from Mountaintop Fire Lookout Stations in Determining Atmospheric Stability. Jonathan W. Corey, April 1979. (PB298899/AS)
143 The Depth of the Marine Layer at San Diego as Related to Subsequent Cool Season Precipitation Episodes in Arizona. Ira S. Brenner, May 1979. (PB298817/AS)
144 Arizona Cool Season Climatological Surface Wind and Pressure Gradient Study. Ira S. Brenner, May 1979. (PB298900/AS)
146 The BART Experiment. Morris S. Webb, October 1979. (PB80 155112)
147 Occurrence and Distribution of Flash Floods in the Western Region. Thomas L. Dietrich, December 1979. (PB80 160344)
149 Misinterpretations of Precipitation Probability Forecasts. Allan H. Murphy, Sarah Lichtenstein, Baruch Fischhoff, and Robert L. Winkler, February 1980. (PB80 174576)
150 Annual Data and Verification Tabulation - Eastern and Central North Pacific Tropical Storms and Hurricanes 1979. Emil B. Gunther and Staff, EPHC, April 1980. (PB80 220486)
151 NMC Model Performance in the Northeast Pacific. James E. Overland, PMEL-ERL, April 1980. (PB80 196033)
152 Climate of Salt Lake City, Utah. Wilbur E. Figgins (Retired) and Alexander R. Smith. Fifth Revision, July 1992. (PB92 220177)
153 An Automatic Lightning Detection System in Northern California. James E. Rea and Chris E. Fontana, June 1980. (PB80 225592)
154 Regression Equation for the Peak Wind Gust 6 to 12 Hours in Advance at Great Falls During Strong Downslope Wind Storms. Michael J. Oard, July 1980. (PB91 108367)
155 A Raininess Index for the Arizona Monsoon. John H. Ten Harkel, July 1980. (PB81 106494)
156 The Effects of Terrain Distribution on Summer Thunderstorm Activity at Reno, Nevada. Christopher Dean Hill, July 1980. (PB81 102501)
157 An Operational Evaluation of the Scofield/Oliver Technique for Estimating Precipitation Rates from Satellite Imagery. Richard Ochoa, August 1980. (PB81 108227)
158 Hydrology Practicum. Thomas Dietrich, September 1980. (PB81 134033)
159 Tropical Cyclone Effects on California. Arnold Court, October 1980. (PB81 133779)
160 Eastern North Pacific Tropical Cyclone Occurrences During Intraseasonal Periods. Preston W. Leftwich and Gail M. Brown, February 1981. (PB81 205494)
161 Solar Radiation as a Sole Source of Energy for Photovoltaics in Las Vegas, Nevada, for July and December. Darryl Randerson, April 1981. (PB81 224503)
162 A Systems Approach to Real-Time Runoff Analysis with a Deterministic Rainfall-Runoff Model. Robert J.C. Burnash and R. Larry Ferral, April 1981. (PB81 224495)
163 A Comparison of Two Methods for Forecasting Thunderstorms at Luke Air Force Base, Arizona. LTC Keith R. Cooley, April 1981. (PB81 225393)
164 An Objective Aid for Forecasting Afternoon Relative Humidity Along the Washington Cascade East Slopes. Robert S. Robinson, April 1981. (PB81 23078)
165 Annual Data and Verification Tabulation, Eastern North Pacific Tropical Storms and Hurricanes 1980. Emil B. Gunther and Staff, May 1981. (PB82 230336)
166 Preliminary Estimates of Wind Power Potential at the Nevada Test Site. Howard G. Booth, June 1981. (PB82 127036)
167 ARAP User's Guide. Mark Mathewson, July 1981, Revised September 1981. (PB82 196783)
168 Forecasting the Onset of Coastal Gales Off Washington-Oregon. John R. Zimmerman and William D. Burton, August 1981. (PB82 127051)
169 A Statistical-Dynamical Model for Prediction of Tropical Cyclone Motion in the Eastern North Pacific Ocean. Preston W. Leftwich, Jr., October 1981. (PB82195298)
170 An Enhanced Plotter for Surface Airways Observations. Andrew J. Spry and Jeffrey L. Anderson, October 1981. (PB82 153883)
171 Verification of 72-Hour 500-MB Map-Type Predictions. R.F. Quiring, November 1981. (PB82 158098)
172 Forecasting Heavy Snow at Wenatchee, Washington. James W. Holcomb, December 1981. (PB82 177783)
173 Central San Joaquin Valley Type Maps. Thomas R. Crossan, December 1981. (PB82 196064)
174 ARAP Test Results. Mark A. Mathewson, December 1981. (PB82 198103)
176 Approximations to the Peak Surface Wind Gusts from Desert Thunderstorms. Darryl Randerson, June 1982. (PB82 253089)
177 Climate of Phoenix, Arizona. Robert J. Schmidli, April 1969 (Revised December 1986). (PB87 142063/AS)
178 Annual Data and Verification Tabulation, Eastern North Pacific Tropical Storms and Hurricanes 1982. E.B. Gunther, June 1983. (PB85 106078)
179 Stratified Maximum Temperature Relationships Between Sixteen Zone Stations in Arizona and Respective Key Stations. Ira S. Brenner, June 1983. (PB83 249904)
180 Standard Hydrologic Exchange Format (SHEF) Version I. Phillip A. Pasteris, Vernon C. Bissel, David G. Bennett, August 1983. (PB85 106052)
181 Quantitative and Spacial Distribution of Winter Precipitation along Utah's Wasatch Front. Lawrence B. Dunn, August 1983. (PB85 106912)
182 500 Millibar Sign Frequency Teleconnection Charts - Winter. Lawrence B. Dunn, December 1983. (PB85 106276)
183 500 Millibar Sign Frequency Teleconnection Charts - Spring. Lawrence B. Dunn, January 1984. (PB85 111367)
184 Collection and Use of Lightning Strike Data in the Western U.S. During Summer 1983. Glenn Rasch and Mark Mathewson, February 1984. (PB85 110534)
185 500 Millibar Sign Frequency Teleconnection Charts - Summer. Lawrence B. Dunn, March 1984. (PB85 111359)
186 Annual Data and Verification Tabulation eastern North Pacific Tropical Storms and Hurricanes 1983. E.B. Gunther, March 1984. (PB85 109635)
187 500 Millibar Sign Frequency Teleconnection Charts - Fall. Lawrence B. Dunn, May 1984. (PB85 110930)
188 The Use and Interpretation of Isentropic Analyses. Jeffrey L. Anderson, October 1984. (PB85 132694)
189 Annual Data & Verification Tabulation Eastern North Pacific Tropical Storms and Hurricanes 1984. E.B. Gunther and R.L. Cross, April 1985. (PB85 1878887AS)
190 Great Salt Lake Effect Snowfall: Some Notes and An Example. David M. Carpenter, October 1985. (PB86 119153/AS)
191 Large Scale Patterns Associated with Major Freeze Episodes in the Agricultural Southwest. Ronald S. Hamilton and Glenn R. Lussky, December 1985. (PB86 144474AS)
192 NWR Voice Synthesis Project: Phase I. Glen W. Sampson, January 1986. (PB86 145604/AS)
193 The MCC - An Overview and Case Study on Its Impact in the Western United States. Glenn R. Lussky, March 1986. (PB86 170651/AS)
194 Annual Data and Verification Tabulation Eastern North Pacific Tropical Storms and Hurricanes 1985. E.B. Gunther and R.L. Cross, March 1986. (PB86 170941/AS)
195 Radid Interpretation Guidelines. Roger G. Pappas, March 1986. (PB86 177680/AS)
196 A Mesoscale Convective Complex Type Storm over the Desert Southwest. Darryl Randerson, April 1986. (PB86 190998/AS)
197 The Effects of Eastern North Pacific Tropical Cyclones on the Southwestern United States. Walter Smith, August 1986. (PB87 106258AS)
198 Preliminary Lightning Climatology Studies for Idaho. Christopher D. Hill, Carl J. Gorski, and Michael C. Conger, April 1987. (PB87 180196/AS)
199 Heavy Rains and Flooding in Montana: A Case for Slantwise Convection. Glenn R. Lussky, April 1987. (PB87 185229/AS)
200 Annual Data and Verification Tabulation Eastern North Pacific Tropical Storms and Hurricanes 1986. Roger L. Cross and Kenneth B. Mielke, September 1987. (PB88 110895/AS)
201 An Inexpensive Solution for the Mass Distribution of Satellite Images. Glen W. Sampson and George Clark, September 1987. (PB88 114038/AS)
202 Annual Data and Verification Tabulation Eastern North Pacific Tropical Storms and Hurricanes 1987. Roger L. Cross and Kenneth B. Mielke, September 1988. (PB88 101935/AS)
203 An Investigation of the 24 September 1986 "Cold Sector" Tornado Outbreak in Northern California. John P. Monteverdi and Scott A. Braun, October 1988. (PB89 121297/AS)
204 Preliminary Analysis of Cloud-To-Ground Lightning in the Vicinity of the Nevada Test Site. Carven Scott, November 1988. (PB89 128649/AS)
205 Forecast Guidelines For Fire Weather and Forecasters -- How Nighttime Humidity Affects Wildland Fuels. David W. Goens, February 1989. (PB89 162549/AS)
206 A Collection of Papers Related to Heavy Precipitation Forecasting. Western Region Headquarters, Scientific Services Division, August 1989. (PB89 230833/AS)
207 The Las Vegas McCarran International Airport Microburst of August 8, 1989. Carven A. Scott, June 1990. (PB90-240268)
208 Meteorological Factors Contributing to the Canyon Creek Fire Blowup, September 6 and 7, 1988. David W. Goens, June 1990. (PB90-245085)
209 Stratus Surge Prediction Along the Central California Coast. Peter Felsch and Woodrow Whitlatch, December 1990. (PB91-129239)
210 Hydrotools. Tom Egger. January 1991. (PB91-151787/AS)
211 A Northern Utah Soaker. Mark E. Struthwolf, February 1991. (PB91-168716)
212 Preliminary Analysis of the San Francisco Rainfall Record: 1849-1990. Jan Null, May 1991. (PB91-208439)
213 Idaho Zone Preformat, Temperature Guidance, and Verification. Mark A. Mollner, July 1991. (PB91-227405/AS)
214 Emergency Operational Meteorological Considerations During an Accidental Release of Hazardous Chemicals. Peter Mueller and Jerry Galt, August 1991. (PB91-235424)
215 WeatherTools. Tom Egger, October 1991. (PB93-184950)
216 Creating MOS Equations for RAWS Stations Using Digital Model Data. Dennis D. Gettman, December 1991. (PB92-131473/AS)
217 Forecasting Heavy Snow Events in Missoula, Montana. Mike Richmond, May 1992. (PB92-196104)
218 NWS Winter Weather Workshop in Portland, Oregon. Various Authors, December 1992. (PB93-146785)
219 A Case Study of the Operational Usefulness of the Sharp Workstation in Forecasting a Mesocyclone-Induced Cold Sector Tornado Event in California. John P. Monteverdi, March 1993. (PB93-178697)
220 Climate of Pendleton, Oregon. Claudia Bell, August 1993. (PB93-227536)
221 Utilization of the Bulk Richardson Number, Helicity and Sounding Modification in the Assessment of the Severe Convective Storms of 3 August 1992. Eric C. Evenson, September 1993. (PB94-131943)
222 Convective and Rotational Parameters Associated with Three Tornado Episodes in Northern and Central California. John P. Monteverdi and John Quadros, September 1993. (PB94-131943)
223 Climate of San Luis Obispo, California. Gary Ryan, February 1994. (PB94-162062)
224 Climate of Wenatchee, Washington. Michael W. McFarland, Roger G. Buckman, and Gregory E. Matzen, March 1994. (PB94-164308)
225 Climate of Santa Barbara, California. Gary Ryan, December 1994.
226 Climate of Yakima, Washington. Greg DeVoir, David Hogan, and Jay Neher, December 1994.
227 Climate of Kalispell, Montana. Chris Maier, December 1994.
228 Forecasting Minimum Temperatures in the Santa Maria Agricultural District. Wilfred Pi and Peter Felsch, December 1994.

NOAA SCIENTIFIC AND TECHNICAL PUBLICATIONS

The National Oceanic and Atmospheric Administration was established as part of the Department of Commerce on October 3, 1970. The mission responsibilities of NOAA are to assess the socioeconomic impact of natural and technological changes in the environment and to monitor and predict the state of the solid Earth, the oceans and their living resources, the atmosphere, and the space environment of the Earth.

The major components of NOAA regularly produce various types of scientific and technical information in the following kinds of publications.

PROFESSIONAL PAPERS--Important definitive research results, major techniques, and special investigations.

CONTRACT AND GRANT REPORTS--Reports prepared by contractors or grantees under NOAA sponsorship.

ATLAS--Presentation of analyzed data generally in the form of maps showing distribution of rainfall, chemical and physical conditions of oceans and atmosphere, distribution of fishes and marine mammals, ionospheric conditions, etc.

TECHNICAL SERVICE PUBLICATIONS--Reports containing data, observations, instructions, etc. A partial listing includes data serials; prediction and outlook periodicals; technical manuals, training papers, planning reports, and information serials; and miscellaneous technical publications.

TECHNICAL REPORTS--Journal quality with extensive details, mathematical developments, or data listings.

TECHNICAL MEMORANDUMS--Reports of preliminary, partial, or negative research or technology results, interim instructions, and the like.

Information on availability of NOAA publications can be obtained from:

NATIONAL TECHNICAL INFORMATION SERVICE

U. S. DEPARTMENT OF COMMERCE

5285 PORT ROYAL ROAD

SPRINGFIELD, VA 22161